
Reverse Diffusion Sequential Monte Carlo Samplers

Luhuan Wu*
Columbia University

Yi Han
Columbia University

Christian A. Naesseth
University of Amsterdam

John P. Cunningham
Columbia University

Abstract

We propose a novel sequential Monte Carlo (SMC) method for sampling from unnormalized target distributions based on a reverse denoising diffusion process. While recent diffusion-based samplers simulate the reverse diffusion using approximate score functions, they can suffer from accumulating errors due to time discretization and imperfect score estimation. In this work, we introduce a principled SMC framework that formalizes diffusion-based samplers as proposals while systematically correcting for their biases. The core idea is to construct informative intermediate target distributions that progressively steer the sampling trajectory toward the final target distribution. Although ideal intermediate targets are intractable, we develop *exact approximations* using quantities from the score estimation-based proposal, without requiring additional model training or inference overhead. The resulting sampler, termed *Reverse Diffusion Sequential Monte Carlo*, enables consistent sampling and unbiased estimation of the target’s normalization constant under mild conditions. We demonstrate the effectiveness of our method on a range of synthetic targets and real-world Bayesian inference problems.²

1 Introduction

Sampling from unnormalized target distributions is a fundamental problem in many applications, ranging from Bayesian inference [1, 2] to simulating molecular systems [3]. Classical methods like Markov chain Monte Carlo (MCMC) simulate a Markov chain with the target as its stationary distribution, but they can suffer from slow mixing and difficulty traversing between modes for complex distributions. Particle methods such as importance sampling generate exact samples in a large compute limit; yet they struggle with the curse of dimensionality [4]. Alternatively, variational inference (VI) [5] casts inference as an optimization task, though its success depends on the expressiveness of the variational family and the complexity of the optimization landscape.

Recently, diffusion models have emerged as a powerful approach for sampling from complex distributions [6, 7]. They define a forward noising process that gradually transforms a complex target distribution into a simple base distribution. A reverse denoising process then reconstructs target samples by simulating the dynamics backward in time, starting from the base distribution and guided by a time-dependent score function. In the generative modeling setting, this score function is approximated by a neural network trained on samples from the target distribution. However, in the sampling context, such training data are unavailable and only an unnormalized target density is accessible.

Recent works on diffusion-based samplers explore alternative ways to approximate the score function directly from the target density, enabling sampling without access to training data. One line of works, known as *diffusion Monte Carlo (MC) samplers*, estimates the score function using MC methods.

*Correspondence email: lw2827@columbia.edu

²Our code is available at <https://github.com/LuhuanWu/RDSMC>.

Huang et al. [8], Grenioux et al. [9] consider Langevin-style MC algorithms, but they rely on a good initialization of the reverse diffusion process to ensure theoretical guarantees. He et al. [10] propose an alternative scheme based on rejection sampling which relaxes prior assumptions and improves sampling efficiency in low-dimensional regimes. These approaches demonstrate both theoretical and empirical advantages over conventional MCMC methods, particularly for multi-modal distributions.

In contrast to relying on MC estimation during sampling time, a complementary line of research trains a neural network in advance to approximate the score function. To this end, some works propose new score matching objectives [11, 12, 13], while variational approaches instead optimize divergences between forward and reverse diffusion processes [14, 15, 16, 17, 18].

While promising, diffusion-based samplers suffer from two sources of bias: discretization error in simulating the reverse diffusion process and approximation error in the estimated or learned score function. An exception is Phillips et al. [11] which mitigates the bias of a *trained* diffusion-based sampler using Sequential Monte Carlo (SMC), a general inference tool for sequential models [19, 20]. However, such training-based methods remain computationally complex compared to classical sampling methods and often rely on special neural network preconditioning [21].

To address these challenges, we develop a new diffusion-based sampler, *Reverse Diffusion Sequential Monte Carlo* (RDSMC) for sampling from unnormalized target distributions, which is training-free and admits theoretical guarantees. Inspired by prior work, we formalize diffusion MC samplers as proposal mechanisms within an SMC framework. At a high level, RDSMC generates multiple *particles* from the reverse diffusion dynamics using MC-based score estimates. To correct the bias in proposals, we introduce intermediate target distributions that guide resampling of particles at each step, progressively steering them toward the final target distribution of interest.

Crucially, our intermediate targets are efficiently computed using byproducts of MC-based score estimates, incurring no additional cost. Moreover, they form an *exact approximation* to the ideal intermediate targets that maximize sampling efficiency, defined by the marginal distributions of an extended final target [19, 22]. This design helps particles stay closely aligned with the final target throughout the sampling process. In contrast, Phillips et al. [11] learn neural network-based surrogates that require additional training and attain the ideal target only at the final step.

RDSMC belongs to a class of nested SMC methods [23, 24], inheriting the standard SMC guarantees. In particular, it produces asymptotically exact samples from the target in the limit of many particles, and provides an unbiased estimate of the normalization constant for any fixed size of particles.

Our contributions are summarized as follows:

- We propose a new SMC algorithm, Reverse Diffusion Sequential Monte Carlo (RDSMC), based on the reverse diffusion process for sampling from unnormalized distributions.
- RDSMC is training-free and extends existing diffusion MC samplers to achieve asymptotically exact sampling and provide unbiased estimates of the normalization constant, while incurring almost no computational overhead given the same number of final samples.
- Empirically, RDSMC outperforms or matches existing diffusion MC samplers and classical geometric annealing-based Annealed Importance Sampling (AIS) [25] and SMC samplers [26] on synthetic targets and Bayesian logistic regression benchmarks.

2 Background

Diffusion models. Diffusion models [6, 7] evolve a complex target distribution $\pi(x)$ into a simple base distribution $\pi_1(x)$, e.g. $\pi_1(x) = \mathcal{N}(0, 1)$, via a forward stochastic differential equation (SDE)

$$dx_t = f(t)x_t dt + g(t)dB_t, \quad t : 0 \rightarrow 1, \quad (1)$$

where $f(t)$ and $g(t)$ are the drift and diffusion coefficients, and B_t is the standard Brownian motion.

To generate samples from $\pi(x)$, we simulate a reverse SDE initialized from $x_1 \sim \pi_1(x)$,

$$dx_t = [f(t)x_t - g(t)^2 \nabla_{x_t} \log \pi_t(x_t)] dt + g(t)d\bar{B}_t, \quad t : 1 \rightarrow 0, \quad (2)$$

where $\nabla_{x_t} \log \pi_t(x_t)$ is the score function of the marginal density $\pi_t(x_t)$ at time t induced by the forward process in Eq. (1), and \bar{B}_t is the reverse-time Brownian motion.

Diffusion MC samplers. Building on the diffusion model paradigm, recent works use MC methods to simulate the reverse dynamics in Eq. (2) whose terminal distribution corresponds to the target distribution $\pi \propto \tilde{\pi}$ of interest [8, 9, 10]. While the score function $\nabla_{x_t} \log \pi_t(x_t)$ is generally intractable, the key idea is to construct MC estimates via the denoising score identity [DSI, 27, 28],

$$\nabla_{x_t} \log \pi_t(x_t) = \int \frac{\alpha(t)x_0 - x_t}{\sigma(t)^2} \pi(x_0 | x_t) dx_0, \quad (3)$$

where $\pi(x_0 | x_t) \propto \tilde{\pi}(x_0) \mathcal{N}(x_0 | \alpha(t)x_0, \sigma(t)^2 \mathbb{I})$ is the *denoising posterior*, which treats the unnormalized target $\tilde{\pi}(x_0)$ as the prior and the forward transition density $\mathcal{N}(x_0 | \alpha(t)x_0, \sigma(t)^2 \mathbb{I})$ from Eq. (1) as the likelihood. The coefficients $\alpha(t)$ and $\sigma(t)$ are determined by the drift and diffusion terms $f(t)$ and $g(t)$ (see § A.1 for details).

Eq. (3) suggests that score estimation can be cast as a posterior inference problem. In practice, one can draw approximate samples from the denoising posterior to form an MC estimate of the score, which is then substituted into the reverse dynamics to generate samples from π . Other score identities beyond the DSI can also be leveraged (see § A.2).

Sequential Monte Carlo. SMC [19, 20] is a particle-based method for sampling from a sequence of distributions defined on variables $x_{0:T}$, terminating at a final target distribution of interest. We consider a reverse-time formulation, where SMC evolves a weighted collection of N particles $\{x_t^{(i)}, w_t^{(i)}\}_{i=1}^N$ from $t = T$ to 0, gradually approximating the final target.

An SMC sampler requires two key design choices [19], a sequence of *intermediate proposals*, $q_T(x_T)$ and $\{q_t(x_t | x_{t+1})\}_{t=0}^{T-1}$, and a sequence of (unnormalized) *intermediate target distributions*, $\{\gamma_t(x_{t:T})\}_{t=0}^T$, such that the final target $\gamma_0(x_{0:T})$ recovers the distribution of interest.

SMC initializes N particles $x_T^{(i)} \sim q_T(x_T)$ with weights $w_T^{(i)} \leftarrow \gamma_T(x_T^{(i)})/q_T(x_T^{(i)})$ for $i = 1, \dots, N$. Then for each step $t = T-1, \dots, 0$ and particle $i = 1, \dots, N$, it proceeds as follows:

1. resample ancestor $x_{t+1}^{(i)} \sim \text{Multinomial}(x_{t+1}^{(1:N)}, w_{t+1}^{(1:N)})$;
2. propagate particle $x_t^{(i)} \sim q_t(x_t | x_{t+1}^{(i)})$;
3. compute weight $w_t^{(i)} \leftarrow \gamma_t(x_{t:T}^{(i)}) / [\gamma_{t+1}(x_{t+1:T}^{(i)}) q_t(x_t^{(i)} | x_{t+1}^{(i)})]$.

The final set of weighted particles forms a discrete approximation to the final target γ_0 , which is asymptotically exact given infinite particles under regularity conditions [20]. However, the efficacy of SMC greatly depends on the choice of intermediate targets and proposals – the closer these intermediate distributions are to the marginals of the final target, the more effective the SMC sampler.

3 Method

Our goal is to sample from a target distribution $\pi(x) = \frac{1}{Z} \tilde{\pi}(x)$, where $\tilde{\pi}(x)$ is the unnormalized target and $Z = \int \tilde{\pi}(x) dx$ is a generally intractable normalization constant. We develop Reverse Diffusion Sequential Monte Carlo (RDSMC), a diffusion-based SMC sampler targeting $\pi(x)$.

To enable sequential inference with SMC, we define an *extended target distribution* over a discretized trajectory $x_{0:T} = (x_0, \dots, x_T)$ of the forward process in Eq. (1),

$$\pi(x_{0:T}) = \pi(x_0) \prod_{t=1}^T \pi(x_t | x_{t-1}), \quad (4)$$

where $0 = \tau_0 < \dots < \tau_T = 1$ are $T + 1$ discretization times and $\pi(x_t | x_{t-1})$ is the forward transition density from time τ_{t-1} to τ_t induced by Eq. (1) (see § A.1 for analytical expressions). Without loss of generality, we assume a uniform discretization step size $\delta = 1/T = \tau_t - \tau_{t-1}, \forall t = 1, \dots, T$.

This construction yields a sequence of intermediate targets $\{\pi(x_{t:T})\}_{t=T}^0$, whose final marginal $\pi(x_0)$ recovers the desired target. These intermediate targets provide a natural setting for SMC, and in fact, are *optimal* intermediate targets. However, they are intractable to sample from and to evaluate.

To address this challenge, we develop RDSMC leveraging the dual structure of diffusion processes, generating samples in the reverse direction while grounding their targets in the forward direction. In § 3.1, we introduce a sequence of proposals based on the reverse diffusion process using MC score estimates. To correct the resulting proposal bias, in § 3.2, we develop practical intermediate targets that form *exact approximations* to the optimal targets $\{\pi(x_{t:T})\}_{t=0}^T$ using byproducts of MC score estimates. Finally in § 3.3, we present the full RDSMC algorithm and its theoretical guarantees.

Notation. We slightly abuse notation by letting x_t denote both the continuous-time variable x_t for $t \in [0, 1]$, as used in Eqs. (1) and (2), and the discrete-time variable for $t \in \{0, \dots, T\}$, as used throughout this section. We denote $f_t := f(\tau_t), g_t := g(\tau_t), \alpha_t := \alpha(\tau_t), \sigma_t := \sigma(\tau_t)$ for time-dependent diffusion coefficients from Eqs. (1) and (3). For generality, we define u_t as the collection of *all* auxiliary random variables generated in the MC score estimation at step t .

3.1 Reverse diffusion proposal

We design an extended proposal distribution based on the reverse diffusion process with MC score estimates, jointly modeling diffusion dynamics x_t and auxiliary randomness u_t from score estimation.

MC score estimation. Given a sample x_t at step t , we define a generic MC score estimator $s(x_t, u_t) \approx \nabla_{x_t} \log \pi(x_t)$ based on the DSI in Eq. (3), where u_t is the estimation randomness associated with some sampling distribution $q(u_t | x_t)$.

As an illustrative example, consider an importance sampling (IS) estimator (Algorithm 2) targeting the posterior $\pi(x_0 | x_t) \propto \tilde{\pi}(x_0) \mathcal{N}(x_t | \alpha_t x_0, \sigma_t^2 \mathbb{I})$. We draw M importance samples $u_t^{(m)}$ from the proposal $q(u_t^{(m)} | x_t) := \mathcal{N}(u_t^{(m)} | x_t / \alpha_t, \sigma_t^2 / \alpha_t^2 \mathbb{I})$ for $m = 1, \dots, M$, and estimate the score by

$$\nabla_{x_t} \log \pi(x_t) \approx s(x_t, u_t) := \sum_{m=1}^M \frac{w^{(m)}}{\sum_{m'=1}^M w^{(m')}} \cdot \frac{\alpha_t u_t^{(m)} - x_t}{\sigma_t^2}, \quad (5)$$

which corresponds to an MC approximation of the RHS of Eq. (3). The importance weights $w^{(m)}$ are

$$w^{(m)} = \frac{\tilde{\pi}(u_t^{(m)}) \mathcal{N}(x_t | \alpha_t u_t^{(m)}, \sigma_t^2 \mathbb{I})}{q(u_t^{(m)} | x_t)}, \quad m = 1, \dots, M. \quad (6)$$

In this case, the auxiliary randomness is to the collection of all importance samples $u_t = \{u_t^{(m)}\}_{m=1}^M$.

In practice, we use a more sophisticated AIS scheme to improve the accuracy of score estimates (Algorithm 3). More informative IS proposals or other MC methods such as SMC and rejection sampling may also be used; see § B.1 for further details.

Approximate reverse diffusion dynamics. With the score estimates in place, we approximate the transition kernel of the reverse SDE in Eq. (2) to define a conditional proposal for x_t ,

$$q(x_t | x_{t+1}, u_{t+1}) := \mathcal{N}(x_t | x_{t+1} - [f_{t+1} x_{t+1} - g_{t+1}^2 s(x_{t+1}, u_{t+1})] \delta, g_{t+1}^2 \delta). \quad (7)$$

Extended proposal distributions. The full sampling process starts by drawing x_T from a tractable base distribution $q(x_T)$, e.g. $q(x_T) = \mathcal{N}(0, 1)$. We then iteratively evolve x_t for $t = T-1, \dots, 0$ using the reverse diffusion dynamics $q(x_t | x_{t+1}, u_{t+1})$ in Eq. (7) where auxiliary variable $u_{t+1} \sim q(u_{t+1} | x_{t+1})$ is sampled in previous iteration to estimate the score $s(x_{t+1}, u_{t+1})$.

The overall sampling process defines a proposal over the extended space of $\{x_t, u_t\}_{t=0}^T$,

$$q(x_{0:T}, u_{0:T}) := q(x_T) q(u_T | x_T) \prod_{t=0}^{T-1} q(x_t | x_{t+1}, u_{t+1}) q(u_t | x_t). \quad (8)$$

While sampling u_0 at the final step $t = 0$ is not necessary, we retain it for notation simplicity.

This sampling procedure builds on prior work of Huang et al. [8], Grenioux et al. [9], which estimate the score function using MCMC, and by He et al. [10] which use rejection sampling. We formalize these ideas by defining an extended proposal distribution that incorporates randomness in MC score estimates. In particular, we adopt an IS or AIS-based MC approach that also provides an unbiased estimate of the normalization constant, a property that, in principle, can be achieved by the rejection sampling approach of He et al. [10] as well. This property will be leveraged in the next part to construct intermediate targets for RDSMC.

3.2 Intermediate targets

Samples from the reverse diffusion proposal deviate from the desired target π due to two sources of error: time discretization of the reverse SDE, and bias in score estimation. To correct these errors, we design a series of intermediate target distributions. We first characterize the optimal but intractable targets, and then develop practical approximations using byproducts of score estimation. Finally, we extend the intermediate targets to include auxiliary variables. Our construction aligns with the optimal targets at intermediate steps and recovers the desired marginal $\pi(x_0)$ at the final step $t = 0$.

Optimal intermediate targets. The optimal intermediate target at step t is the marginal distribution of the extended target $\pi(x_{0:T})$ in Eq. (4),

$$\pi(x_{t:T}) = \int \pi(x_{0:T}) dx_{0:t-1} = \pi(x_t) \prod_{i=t+1}^T \pi(x_i | x_{i-1}), \quad (9)$$

as it leads to exact samples from $\pi(x_{0:T})$ when combined with locally optimal proposals [19].

However, the marginal $\pi(x_t) = \int \pi(x_0) \mathcal{N}(x_t | \alpha_t x_0, \sigma_t^2 \mathbb{I}) dx_0$ in Eq. (9) involves an intractable integral, except in the final step $t = 0$, where $\pi(x_0)$ is known up to a normalization constant.

Marginal estimation. For $t > 0$, we approximate the marginal $\pi(x_t)$ by $\hat{\pi}(x_t, u_t)$ using byproducts of MC score estimates, where we recall u_t is the estimation randomness. The key insight is that $Z\pi(x_t)$ is the normalization constant of the posterior $\pi(x_0 | x_t) \propto \tilde{\pi}(x_0) \mathcal{N}(x_t | \alpha_t x_0, \sigma_t^2 \mathbb{I})$, that is,

$$\int \tilde{\pi}(x_0) \mathcal{N}(x_t | \alpha_t x_0, \sigma_t^2 \mathbb{I}) dx_0 = Z \int \pi(x_0) \mathcal{N}(x_t | \alpha_t x_0, \sigma_t^2 \mathbb{I}) dx_0 = Z\pi(x_t).$$

Hence, we can re-use the posterior inference procedure in MC score estimation to obtain an unbiased estimate of the desired marginal $\pi(x_t)$ (up to a factor of Z).

For example, IS or AIS-based score estimation (Algorithms 2 and 3) generates importance weights $\{w^{(m)}\}_{m=1}^M$ targeting $\pi(x_0 | x_t)$ for a fixed x_t ; we then obtain an unbiased marginal estimate

$$\hat{\pi}(x_t, u_t) := \frac{1}{M} \sum_{m=1}^M w^{(m)}, \quad \text{with } \mathbb{E}_{q(u_t | x_t)} [\hat{\pi}(x_t, u_t)] = Z\pi(x_t). \quad (10)$$

At the final step $t = 0$, we set $\hat{\pi}(x_0, u_0) := \tilde{\pi}(x_0) = Z\pi(x_0)$ as no approximation is needed.

Extended intermediate targets. Finally, we incorporate the auxiliary variables u_t by setting their targets to match their sampling distributions and define the extended intermediate target as

$$\gamma_t(x_{t:T}, u_{t:T}) := \hat{\pi}(x_t, u_t) q(u_t | x_t) \prod_{i=t}^{T-1} \pi(x_{i+1} | x_i) q(u_{i+1} | x_{i+1}) \quad (11)$$

for $t = 0, \dots, T-1$, and $\gamma_T(x_T, u_T) := \hat{\pi}(x_T, u_T) q(u_T | x_T)$.

The structure in Eq. (11) mirrors that of the optimal targets in Eq. (9), replacing the intractable marginal $\pi(x_t)$ with an unbiased estimate $\hat{\pi}(x_t, u_t)$ (up to a factor of Z) and accounting for auxiliary randomness $u_{t:T}$. Moreover, we make the following two observations.

Observation 1. The final marginal target at $t = 0$ matches the desired $\pi(x_0)$ with *no approximations*,

$$\begin{aligned} \gamma_0(x_0) &= \int \gamma_0(x_{0:T}, u_{0:T}) dx_{1:T}, u_{0:T} \\ &= \int \hat{\pi}(x_0, u_0) q(u_0 | x_0) \prod_{i=1}^T \pi(x_i | x_{i-1}) q(u_i | x_i) dx_{1:T}, u_{0:T} \\ &= \tilde{\pi}(x_0) \propto \pi(x_0), \end{aligned} \quad (12)$$

as $\hat{\pi}(x_0, u_0) = \tilde{\pi}(x_0)$ by construction. This implies our final SMC target is correctly specified.

Algorithm 1: Reverse Diffusion Sequential Monte Carlo (RDSMC)

Input: Unnormalized target $\tilde{\pi}(x_0)$, number of particles N , discretization steps T (with step size $\delta = 1/T$), diffusion schedule $\{\alpha_t, \sigma_t, f_t, g_t\}$, base distribution $q(x_T)$, and additional inputs for score and marginal estimation η

Output: Weighted samples $\{x_0^{(i)}, w_0^{(i)}\}_{i=1}^N$ and normalization constant estimate \hat{Z}

```
1 for  $i \leftarrow 1$  to  $N$  do
2   Sample  $x_T^{(i)} \sim q(x_T)$ ;
3   Compute score and marginal estimates  $s_T^{(i)}, \hat{\pi}_T^{(i)} \leftarrow \text{Algorithm 3}(\pi, \alpha_T, \sigma_T, x_T^{(i)}, \eta)$ ;
4   Compute weight:  $w_T^{(i)} \leftarrow \frac{\hat{\pi}_T^{(i)}}{q(x_T^{(i)})}$ ;
5 for  $t \leftarrow T-1$  to 0 do
6   Resample  $\{x_{t+1}^{(i)}, u_{t+1}^{(i)}, s_{t+1}^{(i)}, \hat{\pi}_{t+1}^{(i)}\}_{i=1}^N$  according to weights  $\{w_{t+1}^{(i)}\}_{i=1}^N$ ;
7   for  $i \leftarrow 1$  to  $N$  do
8     Sample  $x_t^{(i)} \sim q(x_t | x_{t+1}^{(i)}, u_{t+1}^{(i)}) := \mathcal{N}(x_t | x_{t+1}^{(i)} - [f_{t+1}x_{t+1}^{(i)} - g_{t+1}^2 s_{t+1}^{(i)}] \delta, g_{t+1}^2 \delta)$ ;
9     if  $t > 0$  then
10      Compute score and marginal estimates  $s_t^{(i)}, \hat{\pi}_t^{(i)} \leftarrow \text{Algorithm 3}(\pi, \alpha_t, \sigma_t, x_t^{(i)}, \eta)$ ;
11     else
12      Compute exact marginal  $\hat{\pi}_0^{(i)} \leftarrow \tilde{\pi}(x_0^{(i)})$ ;
13     Compute weight:  $w_t^{(i)} \leftarrow \frac{\hat{\pi}_t^{(i)} \pi(x_{t+1}^{(i)} | x_t^{(i)})}{\hat{\pi}_{t+1}^{(i)} q(x_t^{(i)} | x_{t+1}^{(i)}, u_{t+1}^{(i)})}$ ;
14 Compute normalization constant estimate  $\hat{Z} \leftarrow \prod_{t=0}^T \frac{1}{N} \sum_{i=1}^N w_t^{(i)}$ .
```

Observation 2. Marginalizing out $u_{t:T}$ in $\gamma_t(x_{t:T}, u_{t:T})$ recovers the optimal target $\pi(x_{t:T})$, $\forall t$,

$$\begin{aligned} \int \gamma_t(x_{t:T}, u_{t:T}) du_{t:T} &= \int \hat{\pi}(x_t, u_t) q(u_t | x_t) \prod_{i=t}^{T-1} \pi(x_{i+1} | x_i) q(u_{i+1} | x_{i+1}) du_{t:T} \\ &= \mathbb{E}_{q(u_t | x_t)} [\hat{\pi}(x_t, u_t)] \prod_{i=t}^{T-1} \pi(x_{i+1} | x_i) \\ &= Z \pi(x_t) \prod_{i=t}^{T-1} \pi(x_{i+1} | x_i) \propto \pi(x_{t:T}), \end{aligned} \tag{13}$$

where the last equality follows from the unbiasedness of marginal estimates, as in Eq. (10). This result shows that our intermediate targets $\gamma_t(x_{t:T}, u_{t:T})$ are aligned with the optimal $\pi(x_{t:T})$, despite the approximation in $\hat{\pi}(x_t, u_t)$, a property known as the *exact approximation* [22, 19].

While the generic SMC framework remains valid under alternative choices of intermediate targets, provided that $\gamma_0(x_0) \propto \pi(x_0)$, our construction offers a balance between theoretical correctness and practical efficiency. The marginal estimates $\hat{\pi}(x_t, u_t)$ in our intermediate targets from Eq. (11) act as *twisting* or *look-ahead* functions [19, Chapter 3] that incorporate future information $\pi(x_0)$ into intermediate steps. Together, Observations 1 and 2 ensure that our intermediate targets provide effective guidance throughout the sampling process while recovering the desired target in the end.

3.3 RDSMC: Algorithm and theoretical guarantee

We now derive weighting functions, the final component of RDSMC, which guides the resampling of particles. We then present the complete algorithm and establish its theoretical guarantees.

Weighting functions. Following the standard SMC framework, we define the weighting functions on the extended space $\{x_{t:T}, u_{t:T}\}$ for $t = T-1, \dots, 0$ as ratios of intermediate targets and proposals

$$w_t := \frac{\gamma_t(x_{t:T}, u_{t:T})}{\gamma_{t+1}(x_{t+1:T}, u_{t+1:T}) q(x_t | x_{t+1}, u_{t+1}) q(u_t | x_t)}. \tag{14}$$

Substituting the expressions for γ_t from Eq. (11) and canceling out common terms yields

$$w_t = \frac{\hat{\pi}(x_t, u_t)\pi(x_{t+1}|x_t)}{\hat{\pi}(x_{t+1}, u_{t+1})q(x_t | x_{t+1}, u_{t+1})}. \quad (15)$$

At the initial step T , the weight is $w_T := \frac{\gamma_T(x_T, u_T)}{q(x_T)q(u_T|x_T)} = \frac{\hat{\pi}(x_T, u_T)}{q(x_T)}$ recalling that $\gamma_T(x_T, u_T) = \hat{\pi}(x_T, u_T)q(u_T | x_T)$ by construction.

Notably, although the intermediate targets and proposals involve auxiliary sampling distributions $q(u_t | x_t)$ for score estimation, the weighting functions w_t in Eq. (15) and w_T do *not* depend on their evaluation. Hence, a generic MC sampler can be used while still retaining computable weights, as long as it produces tractable estimates of the score and marginal densities.

The RDSMC algorithm and theoretical guarantees. We summarize the RDSMC algorithm in Algorithm 1. It initializes N particles from a tractable base distribution. Subsequently, the particles are propagated through a reverse diffusion-based proposal, followed by weighting and resampling using intermediate targets. These steps are enabled by running an inner-level MC estimation of the score function and the marginal density. In this work, we use AIS (Algorithm 3) while other methods can be incorporated as well (see § B.1). The final output of RDSMC is a weighted set of samples approximating the target $\pi(x_0)$, along with an estimate of the normalization constant Z .

RDSMC can be viewed as an adaptation of the *nested* SMC framework [23, 24]. The inner-level MC estimation involves a sampling procedure (e.g. AIS) targeting the intractable posterior $\pi(x_0 | x_t)$, which is then used to assign *proper weights* [19, Chapter 4.3] to proposed samples x_t . Consequently, RDSMC inherits the unbiasedness and asymptotic exactness guarantees of nested SMC [23, 19].

Theorem 1 (Informal). *Under regularity conditions, the RDSMC algorithm provides a consistent estimator of the target distribution $\pi(x_0)$ as particle size $N \rightarrow \infty$ and an unbiased estimator of the normalization constant Z for any $N \geq 1$.*

We provide the formal statement and proof in § C.

Theorem 1 shows that RDSMC effectively wraps a diffusion MC-style proposal within an SMC framework, mitigating its bias as the number of particles increases. Moreover, it provides an unbiased estimate of the normalization constant, a property absent in existing diffusion MC methods [8, 9, 10].

The bias correction mechanism of RDSMC arises from two key aspects: (1) the final target of RDSMC is explicitly constructed to match the desired target $\pi(x_0)$, regardless of the discretization scheme or marginal density approximation (Observation 1); and (2) errors in score estimation affect only the proposal steps, which are accounted for in the weighting functions. Therefore, the weighting and resampling steps in the outer SMC loop asymptotically correct for proposal bias, ensuring convergence to the final target $\pi(x_0)$ in the limit of many particles.

4 Related works

Diffusion MC samplers. Huang et al. [8] develop the RDMC sampler based on the reverse diffusion process using Langevin-style MCMC to estimate the score function. They initialize the sampler at some $\tau_T < 1$ via a nested Langevin procedure. Grenioux et al. [9] propose a similar SLIPS sampler with a signal-to-noise-ratio (SNR)-adjusted discretization scheme, and provide further guidance on choosing the initial sampling time τ_T under suitable conditions. In contrast, we use AIS-based score estimators to enable marginal estimation and start sampling from the base distribution at $\tau_T = 1$.

Alternatively, He et al. [10] explore rejection sampling for score estimation, improving the sampling efficiency in low-dimensional settings, which may be incorporated into our framework as well.

While these methods provide certain theoretical guarantees, we offer an orthogonal means to improve their accuracy by increasing the number of particles. RDSMC can be viewed as a generic SMC wrapper around these diffusion-MC samplers (given suitable score estimators), enabling consistent sampling and unbiased estimation of the normalization constant.

Training-based diffusion samplers In addition to developing MC estimates of the score function, another line of work trains a neural network directly using unnormalized target information.

Variational approaches achieve this goal by minimizing the divergence between forward and reverse processes [14, 15, 17, 18, 16], while Akhound-Sadegh et al. [12], OuYang et al. [13] exploit various identities of the score function or a related energy function. Similar to their training-free MC-based counterparts, these methods are prone to discretization and score approximation errors.

Closest to our work is Phillips et al. [11] that also use SMC to correct proposal bias. Their method requires training neural networks, while ours is training-free. Moreover, their neural network-based intermediate targets incur approximation errors except at the last step, while ours reflect the true target marginals at each SMC iteration. See an empirical comparison in § E.5.3.

He et al. [21] show that many training-based methods incur heavy computational overhead compared to classical sampling methods and rely on special network preconditioning. For this reason, we limit our empirical comparison to training-free samplers. Nonetheless, an interesting direction for future work is to combine our method with training-based approaches to further enhance performance.

SMC for conditional generation from diffusion models. Beyond classical sampling tasks, SMC has been applied to conditional generation for pre-trained diffusion models [29, 30, 31, 32]. While these works also combine SMC and diffusion dynamics, a key distinction is the target distribution: they sample from an existing diffusion model prior tilted with a reward function, whereas our setting involves sampling from any (unnormalized) target distribution. As a result, the way diffusion models are used is different, and we require distinct designs for proposals and intermediate targets in SMC.

Nevertheless, RDSMC uses the estimated marginal densities in Eq. (11) as twisting functions to improve SMC sampling efficiency. This strategy is conceptually similar to that of Wu et al. [30], though in a different setting; see § D for further discussion.

5 Experiments

We evaluate RDSMC on a range of synthetic and real-world target distributions, comparing it to SMC [26], AIS [25], SMS [33], RDMC [8], and SLIPS [9]. AIS and SMC operate over a series of geometric interpolations between the target and a Gaussian proposal with MCMC transitions. SMS samples from the target by sequentially denoising equally noised measurements using a Langevin procedure combined with estimated scores. RDMC and SLIPS are described in § 4.

RDSMC uses a variance-preserving diffusion schedule. To evaluate the effectiveness of our intermediate targets and the importance of resampling, we include two ablations: (i) RDSMC (Proposal), which samples directly from the reverse diffusion proposal in Eq. (8) without any weighting or resampling, and (ii) RDSMC (IS), which applies a final IS correction to samples from RDSMC (Proposal).

Baseline methods follow the implementation of Grenioux et al. [9]. Notably, the information about the target variance (or an estimation) is provided to guide the initialization of the baselines SMC, AIS, SMS and SLIPS. In contrast, our method does *not* make use of this extra information.

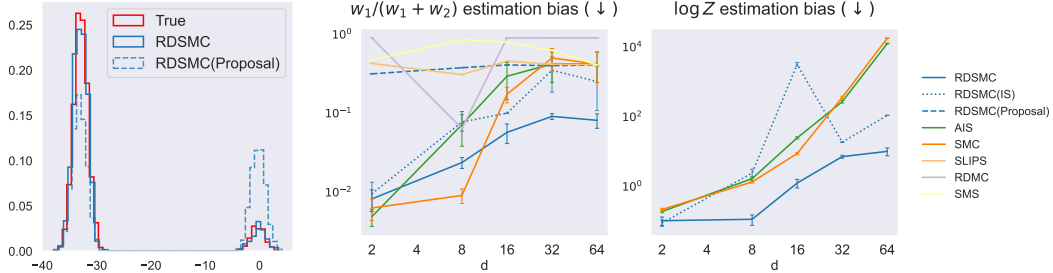
Unless otherwise specified, we use $T = 100$ discretization steps for RDSMC and its variants, and $T = 1,024$ steps for other methods. We generate $N = 4,096$ final samples for all methods, and tune their hyperparameters assuming access to either a validation dataset or an oracle metric.

We provide ablation studies controlling for the discretization steps, the total running time and comparable hyperparameter settings in § E.5, where we observe RDSMC still remains competitive and, in some cases, superior. All experiment details are included in § E.

5.1 Bi-modal gaussian mixtures

We first study bi-modal Gaussian mixtures with an imbalanced weight ratio of $w_1/(w_1 + w_2) = 0.1$ for varying dimensions d . The estimated ratio is obtained by assigning samples to the mode with the highest posterior probability. For each method we select the hyperparameters based on the lowest estimation bias of the weight ratio.

In Figure 1a, we compare the marginal histogram of samples from RDSMC, RDSMC (Proposal), and the true target in $d = 2$. While samples from RDSMC (Proposal) cover both modes, their relative weights are overly balanced. In contrast, RDSMC recovers the calibrated mode weights, indicating the importance of the error correction mechanism by SMC.



(a) $d = 2$: histogram along 1st dimension. While RDSMC’s proposal covers the modes, the SMC procedure is crucial for producing calibrated weights.

(b) Estimation bias of weight ratio $w_1/(w_1 + w_2)$ and log-normalization constant $\log Z$ versus dimension d . Results are averaged over 5 seeds with error bars showing one standard error. Note that SMS, RDMC, and SLIPS do not provide estimate of $\log Z$. For both metrics, the bias increases with d for all methods, while RDSMC outperforms the baselines for most cases.

Figure 1: Bi-modal Gaussian mixture study.

Algorithm	Rings ($d = 2$)		Funnel ($d = 10$)	
	Radius TVD (\downarrow)	$\log Z$ Bias (\downarrow)	Sliced KSD (\downarrow)	$\log Z$ Bias (\downarrow)
AIS	0.10 ± 0.00	0.05 ± 0.00	0.07 ± 0.00	0.28 ± 0.01
SMC	0.10 ± 0.00	0.05 ± 0.00	0.07 ± 0.00	0.28 ± 0.01
SMS	0.24 ± 0.01	N/A	0.15 ± 0.00	N/A
RDMC	0.37 ± 0.00	N/A	0.13 ± 0.00	N/A
SLIPS	0.19 ± 0.00	N/A	0.06 ± 0.00	N/A
RDSMC	0.13 ± 0.01	0.03 ± 0.00	0.11 ± 0.00	0.28 ± 0.10
RDSMC(IS)	0.15 ± 0.01	0.02 ± 0.01	0.33 ± 0.03	1.61 ± 0.14
RDSMC(Proposal)	0.09 ± 0.00	N/A	0.32 ± 0.03	N/A

Table 1: Results on Rings and Funnel (mean \pm standard error over 5 seeds). Bold indicates 95% confidence interval overlap with the best average result. RDSMC has the lowest $\log Z$ estimation bias for both targets. On Rings, RDSMC(Proposal) has the lowest radius TVD, followed by AIS, SMC, and RDSMC. On Funnel, SLIPS has the lowest sliced KSD, followed by AIS, SMC, and RDSMC.

Figure 1b shows the estimation bias of the weight ratio (left), and that of the log-normalization constant $\log Z$ (right). Note that only RDSMC, RDSMC(IS), AIS and SMC provide estimates for $\log Z$. We observe that RDSMC consistently outperforms other methods in both metrics across dimensions. Moreover, RDSMC (Proposal) exhibits consistently high weight ratio estimation bias. While RDSMC (IS) reduces this bias, it still underperforms the full RDSMC procedure, highlighting the effectiveness of intermediate resampling guided by our intermediate target distributions.

In high dimensions, all methods exhibit some degree of mode collapse. RDSMC primarily samples from the dominant mode, resulting in average weight ratio estimation biases of 0.09 and 0.08 for $d = 32$ and 64 , respectively. In contrast, AIS and SMC completely collapse to a single mode, which varies across runs, yielding degenerate estimated ratios of 0 or 1 and an average bias of around 0.4.

5.2 Rings and Funnel distributions

We present results on two additional synthetic targets. Rings, introduced by Grenioux et al. [9], is a 2-dimensional distribution constructed via an inverse polar parameterization: the angular component is uniformly distributed, while the radius component follows a 4-mode Gaussian mixture. Funnel [34], is a 10-dimensional “funnel”-shaped distribution.

For Rings, we assess sample quality using total variational distance in the radius component (Radius TVD). For Funnel, use sliced Kolmogorov-Smirnov distance (Sliced KSD) to evaluate sample quality following Grenioux et al. [9]. As both targets admit tractable normalization constants, we also report the estimation bias for methods that compute them. For each method, we select the hyperparameters with lowest Radius TVD on a heldout validation set for Rings and lowest Sliced KSD for Funnel.

Test LL (\uparrow)	Credit ($d = 25$)	Cancer ($d = 31$)	Ionosphere ($d = 35$)	Sonar ($d = 61$)
AIS	-122.73 ± 0.51	-60.45 ± 0.31	-86.37 ± 0.10	-110.11 ± 0.06
SMC	-123.17 ± 0.05	-60.28 ± 0.11	-86.37 ± 0.10	-110.11 ± 0.06
SMS	-527.79 ± 0.85	-215.64 ± 0.66	-202.56 ± 0.16	-275.44 ± 0.31
RDMC	-388.24 ± 1.75	-182.81 ± 0.43	-108.67 ± 0.09	-128.29 ± 0.03
SLIPS	-121.79 ± 0.04	-56.26 ± 0.08	-85.07 ± 0.07	-102.39 ± 0.03
RDSMC	-124.00 ± 1.96	-62.23 ± 1.96	-87.72 ± 1.75	-101.52 ± 1.84
RDSMC(IS)	-144.38 ± 4.63	-82.47 ± 7.78	-84.90 ± 2.84	-110.57 ± 4.54
RDSMC(Proposal)	-606.03 ± 1.26	-246.86 ± 0.97	-92.62 ± 0.04	-134.72 ± 0.13

Table 2: Bayesian logistic regression with test log-likelihood (mean \pm standard error) averaged over 5 seeds. Bold indicates 95% confidence interval overlap with that of the best average result. SLIPS achieves the best overall performance, while RDSMC matches or closely approaches it. In contrast, RDSMC(Proposal) performs noticeably worse, highlighting the effectiveness of the SMC correction.

As shown in Table 1, RDSMC achieves lower or comparable estimation bias of the log-normalization constant relative to AIS and SMC on both targets. On the lower-dimensional Rings target, RDSMC (Proposal) has the lowest radius TVD, where AIS, SMC and RDSMC closely match. On the more challenging Funnel target, SLIPS achieves the lowest sliced KSD; while RDSMC performs slightly worse, it greatly outperforms its IS and Proposal variants.

5.3 Bayesian logistic regression

Finally, we evaluate inference performance on Bayesian logistic regression models using four datasets. Credit and Cancer [35] involve predicting credit risk and breast cancer recurrence, while Ionosphere [36] and Sonar [37] focus on classifying radar and sonar signals, respectively. The inference is performed on 60% of each dataset, leaving 20% for validation and 20% for testing. Each method is tuned using the validation log-likelihood estimate. We report the test log-likelihood in Table 2.

RDSMC achieves the best or near-best performance across datasets, closely matching SLIPS, which performs the best overall. This comparison suggests that SLIPS’s time discretization and initialization strategy may offer complementary benefits despite lacking systematic error correction. RDSMC (IS) underperforms on Credit and Cancer and exhibits higher variance than RDSMC, while RDSMC (Proposal) performs the worst, again highlighting the importance of the SMC mechanism. Compared to baseline methods, RDSMC shows greater variance, likely due to auxiliary randomness in its nested structure, suggesting a direction for future improvement.

6 Discussion

This paper presents a training-free and diffusion-based SMC sampler, Reverse Diffusion Sequential Monte Carlo (RDSMC), for sampling from unnormalized distributions. By leveraging reverse diffusion dynamics as proposals, we devise informative intermediate targets to correct systematic errors within a principled SMC framework. These components rely on Monte Carlo score estimation, without requiring additional training. Our algorithm provides asymptotically exact samples from the target distribution and a finite-sample unbiased estimate of the normalization constant. Empirical results on both synthetic and Bayesian inference tasks demonstrate competitive or superior performance compared to existing diffusion-based and classical geometric annealing-based samplers.

Limitations and future work. As a nested SMC procedure, RDSMC introduces auxiliary variance. Such variance may be mitigated by enhancing autocorrelation within the MC estimation step [e.g. 38]. In high-dimensional Gaussian mixture experiments, we observe a degree of mode collapse, an issue also seen in other samplers. Potential remedies include partial resampling [39], or using more informed proposals. Our method also relies on oracle metrics for hyperparameter tuning, which aligns with existing works; however, developing a more automated strategy remains an important future direction. Finally, to further improve performance, we can incorporate SNR-adapted discretization schemes and informative initializations, as explored by Grenioux et al. [9], as well as combine our approach with training-based diffusion samplers.

References

- [1] Christophe Andrieu, Nando De Freitas, Arnaud Doucet, and Michael I Jordan. An introduction to mcmc for machine learning. *Machine learning*, 50:5–43, 2003.
- [2] Christian P Robert, George Casella, Christian P Robert, and George Casella. The metropolis—hastings algorithm. *Monte Carlo statistical methods*, pages 267–320, 2004.
- [3] Daan Frenkel and Berend Smit. *Molecular simulation: from algorithms to applications*, 2000.
- [4] Sourav Chatterjee and Persi Diaconis. The sample size required in importance sampling. *The Annals of Applied Probability*, 28(2):1099–1135, 2018.
- [5] David M Blei, Alp Kucukelbir, and Jon D McAuliffe. Variational inference: A review for statisticians. *Journal of the American statistical Association*, 112(518):859–877, 2017.
- [6] Jonathan Ho, Ajay Jain, and Pieter Abbeel. Denoising diffusion probabilistic models. *Advances in neural information processing systems*, 33:6840–6851, 2020.
- [7] Yang Song, Jascha Sohl-Dickstein, Diederik P Kingma, Abhishek Kumar, Stefano Ermon, and Ben Poole. Score-based generative modeling through stochastic differential equations. *arXiv preprint arXiv:2011.13456*, 2020.
- [8] Xunpeng Huang, Hanze Dong, Yifan Hao, Yi-An Ma, and Tong Zhang. Reverse diffusion monte carlo. *arXiv preprint arXiv:2307.02037*, 2023.
- [9] Louis Grenioux, Maxence Noble, Marylou Gabri e, and Alain Oliviero Durmus. Stochastic localization via iterative posterior sampling. *arXiv preprint arXiv:2402.10758*, 2024.
- [10] Ye He, Kevin Rojas, and Molei Tao. Zeroth-order sampling methods for non-log-concave distributions: Alleviating metastability by denoising diffusion. *arXiv preprint arXiv:2402.17886*, 2024.
- [11] Angus Phillips, Hai-Dang Dau, Michael John Hutchinson, Valentin De Bortoli, George Deligiannidis, and Arnaud Doucet. Particle denoising diffusion sampler. In *Forty-first International Conference on Machine Learning*, 2024.
- [12] Tara Akhound-Sadegh, Jarrid Rector-Brooks, Avishek Joey Bose, Sarthak Mittal, Pablo Lemos, Cheng-Hao Liu, Marcin Sendera, Siamak Ravanbakhsh, Gauthier Gidel, Yoshua Bengio, et al. Iterated denoising energy matching for sampling from boltzmann densities. *arXiv preprint arXiv:2402.06121*, 2024.
- [13] RuiKang OuYang, Bo Qiang, Zixing Song, and Jos e Miguel Hern andez-Lobato. Bnem: A boltzmann sampler based on bootstrapped noised energy matching. *arXiv preprint arXiv:2409.09787*, 2024.
- [14] Qinsheng Zhang and Yongxin Chen. Path Integral Sampler: a stochastic control approach for sampling. In *The Tenth International Conference on Learning Representations*, 2022.
- [15] Julius Berner, Lorenz Richter, and Karen Ullrich. An optimal control perspective on diffusion-based generative modeling. *Transactions on Machine Learning Research*, 2023.
- [16] Lorenz Richter, Julius Berner, and Guan-Hong Liu. Improved sampling via learned diffusions. In *ICML Workshop on New Frontiers in Learning, Control, and Dynamical Systems*, 2023.
- [17] Francisco Vargas, Will Sussman Grathwohl, and Arnaud Doucet. Denoising diffusion samplers. In *The Eleventh International Conference on Learning Representations*, 2023.
- [18] Francisco Vargas, Shreyas Padhy, Denis Blessing, and Nikolas N usken. Transport meets variational inference: Controlled monte carlo diffusions. In *The Twelfth International Conference on Learning Representations*, 2024.
- [19] Christian A Naesseth, Fredrik Lindsten, Thomas B Sch on, et al. Elements of sequential monte carlo. *Foundations and Trends  in Machine Learning*, 12(3):307–392, 2019.

- [20] Nicolas Chopin and Omiros Papaspiliopoulos. *An introduction to sequential Monte Carlo*. Springer, 2020.
- [21] Jiajun He, Yuanqi Du, Francisco Vargas, Dinghuai Zhang, Shreyas Padhy, RuiKang OuYang, Carla Gomes, and José Miguel Hernández-Lobato. No trick, no treat: Pursuits and challenges towards simulation-free training of neural samplers. *arXiv preprint arXiv:2502.06685*, 2025.
- [22] Christophe Andrieu, Arnaud Doucet, and Roman Holenstein. Particle markov chain monte carlo methods. *Journal of the Royal Statistical Society Series B: Statistical Methodology*, 72(3): 269–342, 2010.
- [23] Christian Naesseth, Fredrik Lindsten, and Thomas Schon. Nested sequential monte carlo methods. In *International Conference on Machine Learning*, pages 1292–1301. PMLR, 2015.
- [24] Christian A Naesseth, Fredrik Lindsten, and Thomas B Schön. High-dimensional filtering using nested sequential monte carlo. *IEEE Transactions on Signal Processing*, 67(16):4177–4188, 2019.
- [25] Radford M Neal. Annealed importance sampling. *Statistics and computing*, 11:125–139, 2001.
- [26] Pierre Del Moral, Arnaud Doucet, and Ajay Jasra. Sequential monte carlo samplers. *Journal of the Royal Statistical Society Series B: Statistical Methodology*, 68(3):411–436, 2006.
- [27] Pascal Vincent. A connection between score matching and denoising autoencoders. *Neural computation*, 23(7):1661–1674, 2011.
- [28] Bradley Efron. Tweedie’s formula and selection bias. *Journal of the American Statistical Association*, 106(496):1602–1614, 2011.
- [29] Brian L Trippe, Jason Yim, Doug Tischer, Tamara Broderick, David Baker, Regina Barzilay, and Tommi Jaakkola. Diffusion probabilistic modeling of protein backbones in 3D for the motif-scaffolding problem. In *International Conference on Learning Representations*, 2023.
- [30] Luhuan Wu, Brian Trippe, Christian Naesseth, David Blei, and John P Cunningham. Practical and asymptotically exact conditional sampling in diffusion models. *Advances in Neural Information Processing Systems*, 36:31372–31403, 2023.
- [31] Gabriel Cardoso, Yazid Janati El Idrissi, Sylvain Le Corff, and Eric Moulines. Monte carlo guided diffusion for bayesian linear inverse problems. *arXiv preprint arXiv:2308.07983*, 2023.
- [32] Raghav Singhal, Zachary Horvitz, Ryan Teehan, Mengye Ren, Zhou Yu, Kathleen McKeown, and Rajesh Ranganath. A general framework for inference-time scaling and steering of diffusion models. *arXiv preprint arXiv:2501.06848*, 2025.
- [33] Saeed Saremi, Ji Won Park, and Francis Bach. Chain of log-concave markov chains. *arXiv preprint arXiv:2305.19473*, 2023.
- [34] Radford M Neal. Slice sampling. *The annals of statistics*, 31(3):705–767, 2003.
- [35] Robert Nishihara, Iain Murray, and Ryan P Adams. Parallel mcmc with generalized elliptical slice sampling. *The Journal of Machine Learning Research*, 15(1):2087–2112, 2014.
- [36] Vincent G Sigillito, Simon P Wing, Larrie V Hutton, and Kile B Baker. Classification of radar returns from the ionosphere using neural networks. *Johns Hopkins APL Technical Digest*, 10(3): 262–266, 1989.
- [37] R Paul Gorman and Terrence J Sejnowski. Analysis of hidden units in a layered network trained to classify sonar targets. *Neural networks*, 1(1):75–89, 1988.
- [38] George Deligiannidis, Arnaud Doucet, and Michael K Pitt. The correlated pseudomarginal method. *Journal of the Royal Statistical Society Series B: Statistical Methodology*, 80(5): 839–870, 2018.

- [39] Luca Martino, Victor Elvira, and Francisco Louzada. Weighting a resampled particle in sequential monte carlo. In *2016 IEEE Statistical Signal Processing Workshop (SSP)*, pages 1–5. IEEE, 2016.
- [40] Simo Särkkä and Arno Solin. *Applied stochastic differential equations*, volume 10. Cambridge University Press, 2019.
- [41] Valentin De Bortoli, Michael Hutchinson, Peter Wirsberger, and Arnaud Doucet. Target score matching, 2024.
- [42] Jiajun He, Yuanqi Du, Francisco Vargas, Yuanqing Wang, Carla P. Gomes, José Miguel Hernández-Lobato, and Eric Vanden-Eijnden. Feat: Free energy estimators with adaptive transport, 2025.
- [43] Jiajun He, Wenlin Chen, Mingtian Zhang, David Barber, and José Miguel Hernández-Lobato. Training neural samplers with reverse diffusive kl divergence. *arXiv preprint arXiv:2410.12456*, 2024.
- [44] Gareth O Roberts and Richard L Tweedie. Exponential convergence of langevin distributions and their discrete approximations. *Bernoulli*, 2(4):341–363, 1996.
- [45] Radford M Neal. Mcmc using hamiltonian dynamics. *arXiv preprint arXiv:1206.1901*, 2012.
- [46] Maxence Noble, Louis Grenioux, Marylou Gabrié, and Alain Oliviero Durmus. Learned reference-based diffusion sampling for multi-modal distributions. *arXiv preprint arXiv:2410.19449*, 2024.
- [47] Adam Paszke, Sam Gross, Francisco Massa, Adam Lerer, James Bradbury, Gregory Chanan, Trevor Killeen, Zeming Lin, Natalia Gimelshein, Luca Antiga, et al. Pytorch: An imperative style, high-performance deep learning library. *Advances in neural information processing systems*, 32, 2019.
- [48] Louis Grenioux, Alain Oliviero Durmus, Eric Moulines, and Marylou Gabrié. On sampling with approximate transport maps. In *Proceedings of the 40th International Conference on Machine Learning*, volume 202 of *Proceedings of Machine Learning Research*, pages 11698–11733. PMLR, 23–29 Jul 2023.
- [49] Rémi Flamary, Nicolas Courty, Alexandre Gramfort, Mokhtar Z. Alaya, Aurélie Boisbunon, Stanislas Chambon, Laetitia Chapel, Adrien Corenflos, Kilian Fatras, Nemo Fournier, Léo Gautheron, Nathalie T.H. Gayraud, Hicham Janati, Alain Rakotomamonjy, Ievgen Redko, Antoine Rolet, Antony Schutz, Vivien Seguy, Danica J. Sutherland, Romain Tavenard, Alexander Tong, and Titouan Vayer. Pot: Python optimal transport. *Journal of Machine Learning Research*, 22(78):1–8, 2021.

A Background: diffusion models and diffusion-based samplers

A.1 Diffusion models

We review common diffusion schedules used in the literature.

Variance-preserving schedule. In Variance-Preserving (VP) schedule [6], the coefficients of the forward SDE in Eq. (1) are given by

$$f(t) = -\frac{1}{2}b(t), \quad g(t) = \sqrt{b(t)}, \quad (16)$$

where $b(t)$ is a time-dependent function

$$b(t) = b_{\min} + t(b_{\max} - b_{\min}),$$

for some constants $b_{\min} \approx 0 \ll b_{\max}$. For a large value of b_{\max} , the reference distribution is approximately standard normal, $p_1(x) \approx \mathcal{N}(x | 0, 1)$.

By Ito's calculus (see e.g. Särkkä and Solin [40]), one can show that the forward transition density $\pi(x_s | x_t)$ for $1 \geq s > t \geq 0$ is given by

$$\pi(x_s | x_t) = \mathcal{N}\left(x_s \mid \frac{\alpha(s)}{\alpha(t)}x_t, \left(1 - \frac{\alpha^2(s)}{\alpha^2(t)}\right)\mathbb{I}\right),$$

where

$$\alpha(t) = \exp\left(-\frac{1}{2}\int_0^t b(s)ds\right), \quad \sigma(t)^2 = 1 - \exp\left(-\int_0^t b(s)ds\right).$$

Variance-exploding schedule. In Variance-Exploding (VE) schedule [7], the forward SDE coefficients in Eq. (1) are given by

$$f(t) = 0, \quad g(t) = \sqrt{\frac{d\sigma^2(t)}{dt}},$$

where $\sigma(t)$ is a non-negative and monotone increasing function with $\sigma(0) = 0$. Commonly used forms of $\sigma(t)$ include polynomial functions, such as linear, quadratic or exponential schedules. When $\sigma(1)$ is large, the reference distribution can be effectively approximated as $\pi_1(x_1) \approx \mathcal{N}(x_1 | 0, \sigma^2(1))$.

Similarly to the VP case, one can derive the following parameters of the forward transition kernel with $\alpha(t) = 1$ and $\sigma(t)$ is the given non-negative and monotone function.

A.2 Score identities used for diffusion MC samplers

In addition to the DSI from Eq. (3), one may consider the following identities to form alternative MC estimates of the score, given MC samples of $\pi_t(x_0 | x_t)$.

Target score identity (TSI) TSI utilizes known structural properties of the target density, such as estimated gradients, facilitating potentially more accurate and lower-variance score estimations at low-noise settings. Formally, the score function of the noisy target distribution $\pi_t(x)$ under the TSI framework satisfies

$$\nabla_x \log \pi_t(x) = \frac{1}{\alpha(t)} \int \nabla_x \log \pi_t(x_0) \pi_t(x_0 | x) dx_0. \quad (17)$$

TSI and its related alternative have been used in several recent studies to improve score estimation accuracy [41, 11, 12, 42].

Mixed score identity (MSI) To balance the advantages of DSI and TSI across different noise regimes, MSI combines both identities through a convex interpolation. Specifically, MSI favors TSI in the low-noise regime and DSI in the high-noise regime, leveraging both strengths. Formally, MSI is a convex combination of TSI and DSI with coefficients $\frac{\alpha(t)^2}{\alpha(t)^2 + \sigma(t)^2}$ and $\frac{\sigma(t)^2}{\alpha(t)^2 + \sigma(t)^2}$:

$$\nabla_x \log \pi_t(x) = \frac{1}{\alpha(t)^2 + \sigma(t)^2} \int \left(\alpha(t)(x_0 + \nabla_x \log \pi_t(x_0)) - x(t)\right) \pi_t(x_0 | x) dx_0. \quad (18)$$

He et al. [43] leverage MSI to train an implicit generative model that produces samples in a single step, demonstrating improved sample quality and efficiency.

Algorithm 2: Importance Sampling (IS)-based score and marginal estimator

Input: Unnormalized prior $\tilde{\pi}(\cdot)$, likelihood parameters $\{\alpha_t, \sigma_t\}$, data x_t , number of importance samples M , and proposal distribution $q(\cdot | x_t)$ (default: $\mathcal{N}(\cdot | x_t/\alpha_t, \sigma_t^2/\alpha_t^2\mathbb{I})$)

Output: Score estimate $s(x_t, u_t)$ and marginal estimate $\hat{\pi}(x_t, u_t)$.

- 1 **for** $m \leftarrow 1$ **to** M **do**
 - 2 Sample $u_t^{(m)} \sim q(\cdot | x_t)$
 - 3 Compute importance weights $w^{(m)} \leftarrow \frac{\tilde{\pi}(u_t^{(m)})\mathcal{N}(x_t|\alpha_t u_t^{(m)}, \sigma_t^2 I)}{q(u_t^{(m)})}$
 - 4 Denote auxiliary variable $u_t \leftarrow \{u_t^{(m)}\}_{m=1}^M$
 - 5 Compute score estimate $s(x_t, u_t) \leftarrow \sum_{m=1}^M \frac{w^{(m)}}{\sum_{m'=1}^M w^{(m')}} \cdot \frac{\alpha_t u_t^{(m)} - x_t}{\sigma_t^2}$
 - 6 Compute marginal estimate $\hat{\pi}(x_t, u_t) \leftarrow \frac{1}{M} \sum_{m=1}^M w^{(m)}$.
-

B Method details

In this section, we discuss several details of RDSMC, including score and marginal estimation strategies in § B.1, the computational complexity in § B.2, and implementation guidelines in § B.3.

B.1 Score and marginal estimation

In this subsection, we present several score and marginal estimators that can be used within RDSMC, which are based on IS, AIS, SMC and rejection sampling. In our main experiments we use AIS-based estimators.

B.1.1 IS-based estimator

The IS-based estimator is summarized in Algorithm 2, which complements the illustration in § 3.1.

Huang et al. [8] consider a similar importance weighted score estimator (see their Eq 5 in Section 3.3) where the proposal $q(\cdot | x_t) = \mathcal{N}(\cdot | x_t/\alpha_t, \sigma_t^2/\alpha_t^2\mathbb{I})$ is obtained by reversing the forward noising likelihood. While the IS-based score estimator can be inefficient when t is large, Huang et al. [8] leverages Unadjusted Langevin Algorithm (ULA) with IS estimator for initialization; And when t is close to 0, they are able to quickly obtain rough score estimates via the IS approach.

B.1.2 AIS and SMC-based estimator

Algorithm 3 presents an AIS-based approach [25] to construct the score and marginal estimates. AIS introduces a sequence of intermediate unnormalized distributions, smoothly bridging a tractable initial proposal distribution $q(x_0 | x_t)$ to the denoising posterior $\pi(x_0 | x_t) \propto \tilde{\pi}(x_0)\mathcal{N}(x_t | \alpha_t x_0, \sigma_t^2\mathbb{I})$. Under a geometric annealing schedule, intermediate targets are $\nu_k(x_0) \propto q(x_0 | x_t)^{1-\beta_k} \pi(x_0 | x_t)^{\beta_k}$ where $\beta_k = k/n$ for $k = 0, \dots, n$.

Algorithm 3 begins by drawing a set of particles from the proposal distribution $q(x_0 | x_t)$. Then it gradually transitions these particles by running MCMC with a kernel invariant to the intermediate targets $\nu_{k+1}(x_0)$ for $k = 0, \dots, n-1$. In this work we mainly consider Metropolis-Hasting adjusted Langevin dynamics [MALA, 44] and Hamiltonian Monte Carlo [HMC, 45]. At each intermediate step, the algorithm updates the importance weights of each particle based on the ratio of successive intermediate targets.

The final weighted set of particles provides a consistent estimate of the desired posterior, which is utilized to construct a score estimate $s(x_t, u_t)$, where u_t denotes all the randomness in this procedure. Additionally, these weights provide an unbiased estimate of marginal density $\hat{\pi}(x_t, u_t)$, i.e. $\mathbb{E}_{q(u_t|x_t)}[\hat{\pi}(x_t, u_t)] = Z\pi(x_t)$, where $q(x_t | x_t)$ is the sampling distribution of u_t given x_t .

SMC adaption of Algorithm 3. We can adapt Algorithm 3 to an SMC-based procedure by incorporating the resampling mechanism. In this case, the weight update in Algorithm 3 is modified

Algorithm 3: Annealed Importance Sampling (AIS)-based Score and Marginal Estimator

Input: Unnormalized prior $\tilde{\pi}(\cdot)$, likelihood parameters $\{\alpha_t, \sigma_t\}$, data x_t , number of importance samples M , number of annealing steps n , initial proposal distribution $q(\cdot | x_t)$ (default: $\mathcal{N}(\cdot | x_t / \alpha_t, \sigma_t^2 / \alpha_t^2 \mathbb{I})$), and MCMC-related inputs {number of MCMC steps per transition l , MCMC transition kernel \mathcal{T} and MCMC step size δ_{mcmc} }

Output: Score estimate $s(x_t, u_t)$ and marginal estimate $\hat{\pi}(x_t, u_t)$

- 1 Set annealing schedule $\beta_k \leftarrow k/n$ for $k = 0, \dots, n$
 - 2 Set initial target $\nu_1(x_0) \leftarrow q(x_0 | x_t)^{1-\beta_1} \tilde{\pi}(x_0)^{\beta_1} \mathcal{N}(x_t | \alpha_t x_0, \sigma_t^2 \mathbb{I})^{\beta_1}$
 - 3 **for** $m \leftarrow 1$ **to** M **do**
 - 4 Draw initial sample $u_t^{(1,m)} \sim q(\cdot | x_t)$
 - 5 Initialize weight $w^{(m)} \leftarrow \frac{\nu_1(u_t^{(1,m)})}{\nu_0(u_t^{(1,m)})}$
 - 6 **for** $k \leftarrow 2$ **to** n **do**
 - 7 Set the current target $\nu_k(x_0) \propto q(x_0 | x_t)^{1-\beta_k} \tilde{\pi}(x_0)^{\beta_k} \mathcal{N}(x_t | \alpha_t x_0, \sigma_t^2 \mathbb{I})^{\beta_k}$
 - 8 **for** $m \leftarrow 1$ **to** M **do**
 - 9 Update sample $u_t^{(k,m)}$ using MCMC transition targeting ν_k starting from $u_t^{(k-1,m)}$
 - 10 Update weight $w^{(m)} \leftarrow w^{(m)} \frac{\nu_k(u_t^{(k,m)})}{\nu_{k-1}(u_t^{(k,m)})}$
 - 11 Denote auxiliary variable $u_t \leftarrow \{\{u_t^{(k,m)}\}_{m=1}^M\}_{k=1}^n$
 - 12 Compute normalized weights $\tilde{w}^{(m)} \leftarrow \frac{w^{(m)}}{\sum_{m'=1}^M w^{(m'')}}$
 - 13 Compute score estimate $s(x_t, u_t) \leftarrow \sum_{m=1}^M \tilde{w}^{(m)} \frac{\alpha_t u_t^{(k,m)} - x_t}{\sigma_t^2}$
 - 14 Compute marginal density estimate $\hat{\pi}(x_t, u_t) \leftarrow \frac{1}{M} \sum_{m=1}^M w^{(m)}$
-

to the incremental weight computation:

$$w^{(k,m)} \leftarrow \frac{\nu_{k+1}(u_t^{(m)})}{\nu_k(u_t^{(m)})}$$

and the initial weight in Algorithm 3 is denoted by $w^{(1,m)}$, for $m = 1, \dots, M$. With this adjustment, we resample particles $\{u_t^{(m)}\}_{m=1}^M$ in the beginning of each iteration k based on the previous weights $\{w^{(k-1,m)}\}_{m=1}^M$ for $k = 2, \dots, n$. The marginal estimate in Algorithm 3 becomes

$$\hat{\pi}(x_t, u_t) \leftarrow \frac{1}{n} \sum_{k=1}^n \frac{1}{M} \sum_{m=1}^M w^{(k,m)}.$$

The other aspect of Algorithm 3 remains the same.

B.1.3 Rejection sampling (RS)-based estimator

In Algorithm 4, we present a rejection sampling (RS)-based approach, building on prior work of He et al. [10] which propose an RS-based score estimator and develop theoretical guarantees for the resulting diffusion MC sampler. We extend their approach to additionally provide an unbiased marginal density estimate alongside the original score estimate. In principle, this procedure can be used within RDSMC (Algorithm 1) as a replacement for the AIS scheme (Algorithm 3). Future work may explore this direction particularly in low-dimensional settings, as He et al. [10] demonstrate advantages over other score estimators in a non-SMC context.

Notably, rejection sampling requires access to a constant C that upper bounds the ratio of the unnormalized target to the proposal. He et al. [10] use Newton's method to find a proxy of C .

B.1.4 Proposal choices in IS/AIS/SMC/RS-based score estimators.

Algorithms 2 to 4 require specifying an (initial) proposal distribution $q(x_0 | x_t)$. The choice of this proposal is flexible and should ideally approximate the true posterior $\pi(x_0 | x_t)$; the closer it is, the more effective the resulting estimator.

Algorithm 4: Rejection Sampling (RS)–based score and marginal estimator

Input: Unnormalized prior $\tilde{\pi}(\cdot)$, likelihood parameters $\{\alpha_t, \sigma_t\}$, data x_t , number of accepted samples M , proposal $q(\cdot | x_t)$ (default: $\mathcal{N}(\cdot | x_t/\alpha_t, \alpha_t^2/\sigma_t^2\mathbb{I})$), and an upper bound

$$C \geq \sup_{u_t} \tilde{\pi}(u_t) \mathcal{N}(x_t | \alpha_t u_t, \sigma_t^2 I) / q(u_t)$$

Output: Score estimate $s(x_t, u_t)$ and marginal estimate $\hat{\pi}(x_t, u_t)$.

```
1  $m, i \leftarrow 1, 1$ 
2 while  $m \leq M$  do
3   Sample proposal  $v_i \sim q(\cdot | x_t)$ 
4   Compute acceptance ratio  $r \leftarrow \frac{\tilde{\pi}(v_i) \mathcal{N}(x_t | \alpha_t v_i, \sigma_t^2 I)}{C q(v_i)}$ 
5   Draw  $v_i \sim \text{Uniform}(0, 1)$ 
6   if  $v < r$  then
7     Accept sample  $u_t^{(m)} \leftarrow v_i$ 
8      $m \leftarrow m + 1$ 
9    $i \leftarrow i + 1$ 
10  $M_{\text{total}} \leftarrow i - 1$ 
11 Denote auxiliary variable  $u_t \leftarrow \{v_i, v_i\}_{i=1}^{M_{\text{total}}}$ 
12 Compute score estimate:  $s(x_t, u_t) \leftarrow \frac{1}{M} \sum_{m=1}^M \frac{\alpha_t u_t^{(m)} - x_t}{\sigma_t^2}$ 
13 Compute marginal estimate:  $\hat{\pi}(x_t, u_t) \leftarrow C \frac{M}{M_{\text{total}}}$ 
```

In Algorithms 2 to 4, the default initial proposal is obtained by reversing the forward noising likelihood, suggested by prior work [8, 12, 43]. This proposal is effective when the likelihood signal is strong—i.e., when t is close to 0—but becomes less efficient as t increases and the signal weakens.

Alternative strategies include using a Gaussian proposal centered at the current x_t . If additional information about the target distribution is available—such as its mean or covariance—it can be incorporated into the proposal. For instance, one may use a Laplace approximation of the target to construct an approximate posterior, which can be used as a sensible proposal.

B.1.5 Score estimator based on other score identities

In Eq. (5) of the main paper, we derive the score estimator based on the DSI in Eq. (3). Alternative score estimators can be derived based on other score identities.

Based on TSI in Eq. (17), we obtain another estimate:

$$\nabla_{x_t} \log p(x_t) \approx s(x_t, u_t) := \sum_{m=1}^M \frac{w^{(m)}}{\sum_{m'=1}^M w^{(m')}} \cdot \frac{\nabla_{u_t} \log q(u_t^{(m)})}{\alpha_t}, \quad (19)$$

where $\{w^{(m)}, u_t^{(m)}\}_{m=1}^M$ is a weighted system approximating the posterior $\pi(x_0 | x_t)$ using an IS/AIS/SMC procedure.

Or, given MSI in Eq. (18), we have:

$$\nabla_{x_t} \log p(x_t) \approx s(x_t, u_t) := \sum_{m=1}^M \frac{w^{(m)}}{\sum_{m'=1}^M w^{(m')}} \cdot \left(\alpha_t (u_t^{(m)} + \nabla_{u_t} \log q(u_t^{(m)})) - x_t \right). \quad (20)$$

We primarily consider DSI and TSI-based estimators in our experiments.

B.2 Computational complexity

The total computational cost of RDSMC scales linearly with the number of diffusion discretization steps T , the number of particles N , and the cost of each score estimation step.

Specifically, for AIS-based score estimator as described in Algorithm 3, the score estimation cost scales linearly with the number of importance samples M , the number of AIS transition steps n , and

the number of MCMC steps per transition l . The vanilla IS-based score estimator in Algorithm 2 is a special case with $n = 1$ and $l = 1$. Therefore the cost of score estimation per SMC particle per time step $\mathcal{O}(Mnl)$. Consequently, the overall complexity for RDSMC is $\mathcal{O}(NT \cdot Mnl)$.

Among these factors, the operations involving discretization steps T , AIS transition steps n , and MCMC steps l must be processed sequentially due to their time-dependent structure. In contrast, computations over the particles N and the importance samples M are embarrassingly parallel and can be efficiently distributed across parallel compute resources.

B.3 Implementation guidelines

We discuss practical implementation guidelines for RDSMC, including the resampling strategy in § B.3.1, score clipping in § B.3.2 and hyperparameter choices in § B.3.3.

B.3.1 SMC resampling strategy

While the resampling step in RDSMC is crucial for steering particles toward high target probability region, it introduces extra variance in the short term. We discuss several strategies to reduce this added variance.

First, we use systematic resampling, which introduces correlations among resampling indices [19, Chapter 2.2.1].

We also consider start resampling at a later stage of the sampling trajectory. At early steps, the Gaussian likelihood provides weaker conditional information, making posterior inference more challenging [8, 9]. Consequently, both the score estimates and marginal density estimates can be significantly biased or exhibit high variance, especially under limited compute budgets. As a result, the intermediate target distributions in early steps may not be sufficiently informative to enable effective resampling. To mitigate this issue, we delay resampling until a designated step $t_{\text{start-resampling}} < T$, which we treat as a tunable hyperparameter.

For timestep $t < t_{\text{start-resampling}}$, we adopt an effective sample size (ESS)-based criterion to decide whether resampling should be performed at each step – a common strategy in SMC literature [19, Chapter 2.2.2]. The ESS at step t is computed as

$$ESS_t := \frac{\left(\sum_{i=1}^N w_t^{(i)}\right)^2}{\sum_{i=1}^N \left(w_t^{(i)}\right)^2}. \quad (21)$$

We trigger resampling only when the normalized ESS, computed as ESS_t/N , is below a threshold κ_{ess} , another hyperparameter which we fix at 0.3 throughout experiments.

When resampling is skipped (i.e. for $t > t_{\text{start-resampling}}$ or when the normalized ESS is above κ_{ess}), we must adjust the computation of the intermediate weights to ensure the unbiasedness of the log normalization constant estimate [19, Chapter 2.2.3]. For iterations where resampling is not performed, the weight update in Algorithm 1 of Algorithm 1 is replaced by

$$w_t^{(i)} \leftarrow \frac{\bar{w}_{t+1}^{(i)}}{1/N} \cdot \frac{\hat{\pi}_t^{(i)} p(x_{t+1}^{(i)} | x_t^{(i)})}{\hat{\pi}_{t+1}^{(i)} q(x_t^{(i)} | x_{t+1}^{(i)}, u_{t+1}^{(i)})} \quad (22)$$

where $\{\bar{w}_{t+1}^{(i)}\}_{i=1}^N$ are the normalized weights in the previous iteration.

B.3.2 Score clipping

To improve numerical stability, one may consider clipping the score estimates within a pre-specified range. Note that score clipping does not affect our theoretical guarantees provided that regularity conditions hold, as the score estimate is only part of the proposal mechanism.

As observed in prior work [46], score estimates produced by the TSI estimator defined in Eq. (17) can exhibit high variance or have large magnitudes, especially during early steps. Akhound-Sadegh et al. [12] apply score norm clipping when training diffusion samplers where the loss function is based on the TSI. Inspired by their work, we also clip the norm of the score estimates to a maximum of 20

when we use the TSI-based score estimates. In contrast, we do not apply clipping when using the DSI-based score estimator.

B.3.3 Hyperparameter choices

The main hyperparameters of RDSMC are:

Diffusion-related hyperparameters.

- Diffusion parameterization: we use the VP diffusion schedule described in Eq. (16) in this work.
- Time discretization strategy: we use a uniform time discretization grid with $T = 100$ steps, though more informative strategies can be incorporated—such as the SNR-adapted scheme proposed by Grenioux et al. [9].

MC score estimation-related hyperparameters.

- Score estimator type: we use AIS-based score estimator (Algorithm 3), with vanilla IS (Algorithm 2) as a special case. We mainly leverage the DSI (Eq. (5)) to estimate the score in most experiments, while we also use the TSI (Eq. (19)) in Bayesian logistic regression tasks.
- MCMC transition kernel: MALA or HMC.
- M : Number of importance samples used in Monte Carlo score estimation
- n : Number of intermediate distributions, i.e. number of AIS steps; for IS $n = 1$
- δ_{mcmc} : Step size used in the MCMC transition kernel (not used in IS). We manually tune this parameter in the main experiments while we use adaptive step size in ablation studies; see discussion below.
- l : Number of MCMC steps per AIS transition (not used in IS). We use $l = 1$ in all experiments.

SMC-related hyperparameters.

- $t_{\text{start-resampling}}$: Starting time for resampling within the SMC trajectory. No resampling is performed for $t/T > t_{\text{start-resampling}}$.
- κ_{ess} : Normalized effective sample size threshold triggering resampling. When $\kappa_{\text{ess}} = 0$, no resampling is applied throughout, which corresponds to RDSMC (IS) if a final-step weighting is applied and RDSMC (Proposal) otherwise. We set $\kappa_{\text{ess}} = 0.3$ in all experiments for RDSMC.

In the main experiments, we choose score estimator and MCMC kernel types by a coarse grid search, and tune $M, n, \delta_{\text{mcmc}}$ and $t_{\text{start-resampling}}$ in a range of values, using validation metrics. The hyperparameter values are summarized Table 3; see details in § E.1.2.

In the ablation experiments in § E.5, we fix most hyperparameters to reduce the degrees of freedom. We use $T = 100, M = 100, n = 50, m = 1, \kappa_{\text{ess}} = 0.3$, and AIS-based score estimator leveraging the DSI, LG as the MCMC kernel. We also use an *adaptive* MCMC step size δ_{mcmc} , as in Grenioux et al. [9]. When the acceptance rate is too high ($> 76\%$) we increase the step size by 3%, when it is $< 74\%$, we decrease step size by 3%, and otherwise we keep the current step size. Only an initial step size value needs to be specified and then it is adaptively adjusted during the sampling process. The *only* hyperparameter in RDSMC that requires tuning is $t_{\text{start-resampling}}$, which we vary in $\{0, 0.1, \dots, 0.9, 1.0\}$. We observe consistent performance and therefore in practice we would recommend users to start with something similar to this configuration.

C Theoretical guarantees of RDSMC

We formally state the theorem providing sufficient conditions for asymptotic accuracy of RDSMC and unbiasedness of the estimate of the normalization constant. Our proof strategy for asymptotic

accuracy is adapted from Wu et al. [30] and the proof for unbiasedness follows the techniques presented in Naesseth et al. [19].

Theorem 2. *Assume*

- (a) *the first marginal estimate $\hat{\pi}(x_T, u_T)$, and the ratios of subsequent ratio $\hat{\pi}(x_t, u_t)/\hat{\pi}(x_{t+1}, u_{t+1})$ are positive and bounded,*
- (b) *the score estimate $s(x_t, u_t)$ is bounded, and x_t has compact support,*
- (c) *variance increases in the forward noising kernel, i.e. for each t , $g_{t+1}^2 > g_t^2$.*

Then the RDSMC algorithm described in Algorithm 1 provides a consistent estimator of the target distribution $\pi(x_0)$ as particle size $N \rightarrow \infty$ and an unbiased estimator of the normalization constant Z for any $N \geq 1$. More specifically,

- (a) *Let $\mathbb{P}_N = \sum_{i=1}^N w_0^{(i)} \delta_{x_0^{(i)}}$ for weighted particles $\{(x_0^{(i)}, w_0^{(i)})\}_{i=1}^N$ returned by Algorithm 1 with N particles. \mathbb{P}_N converges setwise to $\pi(x_0)$ with probability one, that is for every set A , $\lim_{N \rightarrow \infty} \mathbb{P}_N(A) = \int_A \pi(x_0) dx_0$.*
- (b) *For the estimate for the normalization constant \hat{Z} returned by Algorithm 1, we have $\mathbb{E}\hat{Z} = Z$.*

The assumptions of Theorem 2 are typically satisfied in standard implementations of SMC samplers:

- Assumption (a) can be satisfied by the clipping of the marginal estimates $\hat{\pi}(x_t, u_t)$ within the range $[c, C]$ for some constants $c, C > 0$.
- Assumption (b) by clipping scores estimates as well. Additionally, the compactness of the state space x_t is a standard and commonly adopted assumption in the SMC literature.
- Assumption (c) is mild and typically satisfied in practice. In both VE and VP noising schedules commonly used in diffusion models, the variance of the forward kernel increases with time.

Proof of Theorem 2: We first prove the asymptotic exactness of our sampler and then prove the unbiasedness of the normalization constant estimate.

First, Theorem 3 characterizes a set of conditions under which SMC algorithms converge. We restate this result below in our own notation.

Theorem 3 (Chopin and Papaspiliopoulos [20] – Proposition 11.4). *Let $\{(x_0^{(i)}, w_0^{(i)})\}_{i=1}^N$ be the particles and weights returned at the last iteration of a sequential Monte Carlo algorithm with N particles using multinomial resampling. If each weighting function w_t is positive and bounded, then for every bounded, ν_0 -measurable function ϕ of x_t*

$$\lim_{N \rightarrow \infty} \sum_{i=1}^N w_0^{(i)} \phi(x_0^{(i)}) = \int \phi(x_0) \nu_0(x_0) dx_0.$$

with probability one.

An immediate consequence of Theorem 3 is the setwise convergence of the discrete measures. To apply Theorem 3 to show asymptotic accuracy, it is sufficient to show that the weights at each step are upper bounded, as they are defined through probabilities and hence are positive. Since there is a finite number of steps T , it suffices to show that each w_t is bounded.

The initial weight is defined by

$$w_T = \frac{\hat{\pi}(x_T, u_T)}{q(x_T)},$$

which is bounded by Assumption (a).

The intermediate weights are defined by Eq. (14) such that

$$w_t = \frac{\hat{\pi}(x_t, u_t) \pi(x_{t+1} | x_t)}{\hat{\pi}(x_{t+1}, u_{t+1}) q(x_t | x_{t+1}, u_{t+1})}.$$

We first decompose the weights by

$$\log w_t = \log \frac{\hat{\pi}(x_t, u_t)}{\hat{\pi}(x_{t+1}, u_{t+1})} + \log \frac{\pi(x_{t+1} | x_t)}{q(x_t | x_{t+1}, u_{t+1})}.$$

The boundedness of $\log \frac{\hat{\pi}(x_t, u_t)}{\hat{\pi}(x_{t+1}, u_{t+1})}$ is guaranteed by Assumption (a). We now show the boundedness of $\log \frac{\pi(x_{t+1} | x_t)}{q(x_t | x_{t+1}, u_{t+1})}$. First, note that

$$\pi(x_{t+1} | x_t) = \mathcal{N}(x_{t+1} | x_t + f_t x_t \delta, g_t^2 \delta),$$

and

$$q(x_t | x_{t+1}, u_{t+1}) = \mathcal{N}(x_t | x_{t+1} - [f_{t+1} x_{t+1} - g_{t+1}^2 s(x_{t+1}, u_{t+1})] \delta, g_{t+1}^2 \delta).$$

Let $\hat{\mu}_p = x_{t+1} - f_t x_t \delta$ and $\hat{\mu}_q = x_{t+1} - [f_{t+1} x_{t+1} - g_{t+1}^2 s(x_{t+1}, u_{t+1})] \delta$. We can show that $\|\hat{\mu}_p - \hat{\mu}_q\| = \|f_{t+1} x_{t+1} - f_t x_t - g_{t+1}^2 s(x_{t+1}, u_{t+1})\| \delta$ is bounded, which follows from Assumption (b). The log-ratio then simplifies as

$$\log \frac{\pi(x_{t+1} | x_t)}{q(x_t | x_{t+1}, u_{t+1})} \tag{23}$$

$$= \log \frac{|2\pi g_t^2 I|^{-1/2} \exp\{-(2g_t^2)^{-1} \|x_t - \hat{\mu}_p\|^2\}}{|2\pi g_{t+1}^2 I|^{-1/2} \exp\{-(2g_{t+1}^2)^{-1} \|x_t - \hat{\mu}_q\|^2\}} \tag{24}$$

$$\text{Rearrange and let } C = \log |2\pi g_t^2 I|^{-1/2} / |2\pi g_{t+1}^2 I|^{-1/2} \tag{25}$$

$$= -\frac{1}{2} [g_t^{-2} \|x_t - \hat{\mu}_p\|^2 - g_{t+1}^{-2} \|x_t - \hat{\mu}_q\|^2] + C \tag{26}$$

$$\text{Expand and rearrange } \|x_t - \hat{\mu}_q\|^2 = \|x_t - \hat{\mu}_p\|^2 + 2\langle \hat{\mu}_p - \hat{\mu}_q, x_t - \hat{\mu}_p \rangle + \|\hat{\mu}_p - \hat{\mu}_q\|^2 \tag{27}$$

$$= -\frac{1}{2} [(g_t^{-2} - g_{t+1}^{-2}) \|x_t - \hat{\mu}_p\|^2 - 2g_{t+1}^{-2} \langle \hat{\mu}_p - \hat{\mu}_q, x_t - \hat{\mu}_p \rangle - g_{t+1}^{-2} \|\hat{\mu}_p - \hat{\mu}_q\|^2] + C \tag{28}$$

$$\text{Let } C' = C + \frac{1}{2} g_{t+1}^2 \|\hat{\mu}_p - \hat{\mu}_q\|^2 \text{ and rearrange. Note that } \|\hat{\mu}_p - \hat{\mu}_q\|^2 < \infty \tag{29}$$

$$= -\frac{1}{2} (g_t^{-2} - g_{t+1}^{-2}) \|x_t - \hat{\mu}_p\|^2 + g_{t+1}^{-2} \langle \hat{\mu}_p - \hat{\mu}_q, x_t - \hat{\mu}_p \rangle + C' \tag{30}$$

$$\text{By Cauchy-Schwarz,} \tag{31}$$

$$\leq -\frac{1}{2} (g_t^{-2} - g_{t+1}^{-2}) \|x_t - \hat{\mu}_p\|^2 + g_{t+1}^{-2} \|\hat{\mu}_p - \hat{\mu}_q\| \cdot \|x_t - \hat{\mu}_p\| + C' \tag{32}$$

$$\text{By Assumption (c), } g_t^{-2} - g_{t+1}^{-2} > 0, \tag{33}$$

$$\leq \frac{1}{2} \frac{(g_{t+1}^{-2} \|\hat{\mu}_p - \hat{\mu}_q\|)^2}{g_t^{-2} - g_{t+1}^{-2}} + C' \tag{34}$$

$$= \frac{g_{t+1}^{-4}}{2(g_t^{-2} - g_{t+1}^{-2})} \|\hat{\mu}_p - \hat{\mu}_q\|^2 + C' \tag{35}$$

$$\leq C''. \tag{36}$$

The final line follows from the boundedness of $\|\hat{\mu}_p - \hat{\mu}_q\|$. The above derivation shows that each w_t is bounded, which concludes the proof for the asymptotic exactness of our sampler.

Then we show the unbiasedness of the normalization constant estimate \hat{Z} . Let $a_t^{(i)}$ be the index of $x_t^{(i)}$ and $u_t^{(i)}$ before resampling. With that, \hat{Z} is defined by

$$\hat{Z} = \prod_{t=0}^T \frac{1}{N} \sum_{i=1}^N w_t^{(i)}, \quad \text{where } w_t^{(i)} = \frac{\hat{\pi}_t^{(i)} \pi(x_{t+1}^{(i)} | x_t^{a_t^{(i)}})}{\hat{\pi}_{t+1}^{(i)} q(x_t^{a_t^{(i)}} | x_{t+1}^{(i)}, u_{t+1}^{(i)})}, \quad w_T^{(i)} = \frac{\hat{\pi}_T^{(i)}}{\hat{\pi}(x_T^{a_t^{(i)}})}.$$

Denote the normalized weight by $\widetilde{w}_t^{(i)} = \frac{w_t^{(i)}}{\sum_{i=1}^N w_t^{(i)}}$. The distribution of all random variables generated by the SMC method is then given by

$$\begin{aligned}
& Q(x_{0:T}, u_{0:T}, a_{0:T}) \\
&= \pi(x_t, u_T) p(x_{0:T-1}, u_{0:T-1}, a_{0:T}) \\
&= \pi(x_t^{a_T}, u_T^{a_T}) \pi(x_t, u_T \mid x_T^{a_T}, u_T^{a_T}) \prod_{t=0}^{T-1} p(x_t, u_t \mid x_t^{a_t}, u_t^{a_t}) q(x_t^{a_t} \mid x_{t+1}, u_{t+1}) q(u_t^{a_t} \mid x_t^{a_t}), \\
&= \pi(x_t^{a_T}) \left(\prod_{i=1}^N \frac{w_T^{(i)}}{\sum_{i=1}^N w_T^{(i)}} \right) \prod_{i=1}^N \left[\left(\prod_{t=0}^{T-1} \frac{w_t^{(i)}}{\sum_{i=1}^N w_t^{(i)}} q(x_t^{a_t^i} \mid x_{t+1}^{(i)}, u_{t+1}^{(i)}) \right) \right] \\
&\quad \left[q(u_T^{a_T} \mid x_T^{a_T}) \prod_{t=0}^{T-1} q(u_t^{a_t} \mid x_t^{a_t}) \right].
\end{aligned}$$

By $w_t^{(i)} = \frac{\hat{\pi}_t^{(i)} \pi(x_{t+1}^{(i)} \mid x_t^{a_t^i})}{\hat{\pi}_{t+1}^{(i)} q(x_t^{a_t^i} \mid x_{t+1}^{(i)}, u_{t+1}^{(i)})}$ and $w_T^{(i)} = \frac{\hat{\pi}_T^{(i)}}{q(x_T^{a_T})}$, we have:

$$\begin{aligned}
& Q(x_{0:T}, u_{0:T}, a_{0:T}) \\
&= \left(\prod_{t=0}^T \sum_{i=1}^N w_t^{(i)} \right)^{-1} \hat{\pi}_0^{(1)} \left(\prod_{t=0}^{T-1} \pi(x_{t+1}^{(1)} \mid x_t^{a_t^1}) \right) \\
&\quad \prod_{i=2}^N \hat{\pi}_T^{(i)} \prod_{i=2}^N \left[\left(\prod_{t=0}^{T-1} \widetilde{w}_t^{(i)} q(x_t^{a_t^i} \mid x_{t+1}^{(i)}, u_{t+1}^{(i)}) \right) \right] \left[q(u_T^{a_T} \mid x_T^{a_T}) \prod_{t=0}^{T-1} q(u_t^{a_t} \mid x_t^{a_t}) \right],
\end{aligned}$$

where we plug in $w_t^{(1)}$ and rearrange terms.

By multiplying \hat{Z} , we have:

$$\begin{aligned}
\hat{Z} Q(x_{0:T}, u_{0:T}, a_{0:T}) &= \hat{Z} \left(\prod_{t=0}^T \sum_{i=1}^N w_t^{(i)} \right)^{-1} \hat{\pi}_0^{(1)} \left(\prod_{t=0}^{T-1} \pi(x_{t+1}^{(1)} \mid x_t^{a_t^1}) \right) \\
&\quad \prod_{i=2}^N \left[\hat{\pi}_T^{(i)} \left(\prod_{t=0}^{T-1} \widetilde{w}_t^{(i)} q(x_t^{a_t^i} \mid x_{t+1}^{(i)}, u_{t+1}^{(i)}) \right) \right] \left[q(u_T^{a_T} \mid x_T^{a_T}) \prod_{t=0}^{T-1} q(u_t^{a_t} \mid x_t^{a_t}) \right] \\
&= N^{-T} \hat{\pi}_0^{(1)} q(u_0^{a_0^1} \mid x_0^{a_0^1}) \left(\prod_{t=0}^{T-1} \pi(x_{t+1}^{(1)} \mid x_t^{a_t^1}) q(u_{t+1}^{a_{t+1}^1} \mid x_{t+1}^{a_{t+1}^1}) \right) \\
&\quad \prod_{i=2}^N \left[\hat{\pi}_T^{(i)} q(u_t^{a_t^i} \mid x_t^{a_t^i}) \left(\prod_{t=0}^{T-1} \widetilde{w}_t^{(i)} q(x_t^{a_t^i} \mid x_{t+1}^{(i)}, u_{t+1}^{(i)}) q(u_{t+1}^{a_{t+1}^{(i)}} \mid x_{t+1}^{(i)}) \right) \right],
\end{aligned}$$

where the first equality follows from plugging in Q and the second follows from plugging in \hat{Z} .

The expectation of the normalization constant estimate can be written as

$$\begin{aligned}
\mathbb{E}_Q(\hat{Z}) &= N^{-T} \sum_{a_{0:T}} \int \int \hat{\pi}_0^{(1)} q(u_0^{a_0^1} \mid x_0^{a_0^1}) \left(\prod_{t=0}^{T-1} \pi(x_{t+1}^{(1)} \mid x_t^{a_t^1}) q(u_{t+1}^{a_{t+1}^1} \mid x_{t+1}^{a_{t+1}^1}) \right) \\
&\quad \prod_{i=2}^N \left[\hat{\pi}_T^{(i)} q(u_t^{a_t^i} \mid x_t^{a_t^i}) \left(\prod_{t=0}^{T-1} \widetilde{w}_t^{(i)} q(x_t^{a_t^i} \mid x_{t+1}^{(i)}, u_{t+1}^{(i)}) q(u_{t+1}^{a_{t+1}^{(i)}} \mid x_{t+1}^{(i)}) \right) \right] dx_{0:T} du_{0:T} \\
&= N^{-T} \sum_{a_{0:T}} \int \int \hat{\pi}_0^{(1)} q(u_0^{a_0^1} \mid x_0^{a_0^1}) \left(\prod_{t=0}^{T-1} \pi(x_{t+1}^{(1)} \mid x_t^{a_t^1}) q(u_{t+1}^{a_{t+1}^1} \mid x_{t+1}^{a_{t+1}^1}) \right) dx_{0:T}^1 du_{0:T}^1 \\
&= Z,
\end{aligned}$$

where in the second equality, we marginalize the variables not involved in the particle $x_{0:T}^1$ and $x_{0:T}^{a_{0:T}^1}$. The final equality follows because we are averaging over N^T possible cases of $a_{0:T}^1$ and all are equal to Z , which concludes the proof.

D Comparison to Twisted Diffusion Sampler

In this section, we discuss similarities and differences between RDSMC and Twisted Diffusion Sampler [TDS, 30], which is an SMC method for conditional generation from diffusion models.

Structurally, our method shares similarities with TDS, as both methods use some form of "look-ahead" or "twisting" functions [19, Chapter 3] to improve the efficiency of SMC. These twisting functions introduce future information to intermediate states, promote promising particles through the weighting procedure, and improve the SMC sampling efficiency.

Moreover, the incremental weight expression of both TDS and RDSMC takes the same form (their Eq. (11) v.s. our Eq. (15)):

$$w_t := \frac{\psi(x_t)\gamma_t^0(x_{t:T})}{\psi(x_{t+1})\gamma_t^0(x_{t+1:T})q(x_t | x_{t+1})},$$

where ψ is the twisting function, γ_t^0 is the untwisted intermediate target and q is the proposal. The product $\gamma_t(x_{t:T}) := \psi(x_t)\gamma_t^0(x_{t:T})$ defines a series of *twisted* intermediate targets.

While the expressions of these components are method-specific, the structure of the weighting functions is shared between TDS our RDSMC and follows from the generic twisted SMC framework [19, Chapter 3].

Importantly, this weight construction introduces twisting functions in a telescoping manner such that their approximation errors cancel out over the full trajectory. This property ensures that the final target is correct, and the resulting SMC procedure is asymptotically exact for both TDS and RDSMC.

However, we want to highlight several important *differences* between TDS and RDSMC:

1. **Problem setting:** The problem we address is fundamentally different from that of TDS. TDS is designed to sample from the conditional distribution $p_\theta(x_0 | y) \propto p_\theta(x_0)p(y | x_0)$ given a pretrained diffusion model $p_\theta(x_0)$ and a likelihood model $p(y | x_0)$ with the observation y . As a comparison, our goal is to sample from an arbitrary distribution $\pi(x_0)$, assuming access to its unnormalized density $\tilde{\pi}(x_0)$.
2. **Design of key components:** Due to the difference in settings, our intermediate target distributions, proposal distributions, and twisting functions require different designs. In particular,
 - TDS's twisting function is $p(y | \hat{x}_\theta(x_t))$ (their Eq. (8)), the likelihood evaluated at the denoising prediction $\hat{x}_\theta(x_t)$ by the pretrained model, which approximates the intractable likelihood $p_\theta(y | x_t)$. This twisting function incorporates the observation y into the weighting function (their Eq. (11)). Notably, when $t = 0$, TDS's twisting function recovers the exact likelihood $p(y | x_0)$ and no approximation is involved. Given the twisting function, TDS's intermediate target is $p(y | \hat{x}_\theta(x_t))p_\theta(x_{t:T})$ where $p_\theta(x_{t:T})$ is the distribution under the pretrained diffusion model. The proposal is obtained by adding a term that is the gradient of the twisting function, $\nabla_{x_t} \log p(y | \hat{x}_\theta(x_t))$, to the pretrained diffusion model's transition kernel (see their Eq (9) and (11)).
 - In our case, RDSMC uses the marginal estimate $\hat{\pi}(x_t, u_t)$ (Eq. (10)) as the twisting function, which approximates the exact marginal $\pi(x_t)$. The marginal integrates out the future information in $\pi(x_0)$, thereby encoding the target information into the intermediate weight. We define intermediate targets as $\hat{\pi}(x_t, u_t)\pi(x_{t:T})q(u_{t:T} | x_{t:T})$ (a restatement of Eq. (11)); the product term $\hat{\pi}(x_t, u_t)\pi(x_{t:T})$ is structurally similar to TDS's intermediate target, while we additionally account for MC estimation randomness $q(u_{t:T} | x_{t:T})$. We also utilize twisting function to inform the proposal, that is, we use the score estimate $s(x_t, u_t)$, which is connected to the twisting function / marginal estimate $\hat{\pi}(x_t, u_t)$, to design the proposal in Eq. (8).
3. **Use of auxiliary variables:** Our method introduces auxiliary randomness through the Monte Carlo estimation of the twisting function. Incorporating this randomness places RDSMC in the category of nested SMC methods [23]. In contrast, TDS does not use auxiliary variables and operates more like a standard SMC algorithm, without requiring nested sampling.

E Experiment details

This section provides experimental details and additional results.

§ E.1 describes the implementation and hyperparameter settings for RDSMC and all baseline methods. § E.2 to E.4 present supplementary information and additional results for the target distributions used in the *main* experiments. § E.5 reports *additional* experiments that control for hyperparameters, runtime, and other relevant factors to compare across methods, as well as an empirical comparison to Phillips et al. [11].

Compute resources. All experiments were conducted on a single NVIDIA A100 GPU with 40 GB GPU memory, and accessed between 16 GB and 32 GB of CPU memory, depending on the task. RDSMC and baseline methods are all implemented in PyTorch [47].

E.1 Method and hyperparameter details

We first give an overview of baseline methods we benchmark RDSMC against in § E.1.1. We then describe key hyperparameter settings of our method and competing baselines for the main experiments in § E.1.2.

E.1.1 Summary of baseline methods

AIS [25]. The annealed importance sampling (AIS) algorithm defines a sequence of geometrically annealed distributions $\rho_t(x)$ for $t \in \{0, 1, \dots, T\}$ from an initial proposal $\rho_0(x)$ to the desired target $\rho_T(x) \propto \pi(x)$ as $\rho_t(x) \propto \rho_0(x)^{1-\beta_t} \pi(x)^{\beta_t}$ where $\{\beta_t\}_{t=0}^T$ is an increasing linear schedule with each $\beta_t = t/T$. AIS begins by sampling from the initial proposal $\rho_0(x)$ and proceeds through a sequence of MCMC transitions, each targeting the intermediate distribution $\rho_t(x)$. The resulting weighted samples provide a consistent approximation to the target distribution $\pi(x)$. The complexity of AIS is $\mathcal{O}(NTn)$ for N final samples, T annealing steps, and n MCMC transitions per step.

SMC [26]. Sequential Monte Carlo (SMC) operates on the same sequence of annealed distributions as AIS but differs by performing resampling at certain iterations. In our implementation, we consider both constant resampling at each step and an adaptive strategy based on an ESS threshold κ_{ess} . The complexity of SMC is the same as that of AIS.

RDMC [8]. Reverse diffusion Monte Carlo (RDMC) builds on the time-reversed Ornstein–Uhlenbeck diffusion:

$$dY_t = \{Y_t + 2 \nabla \log p_{t_{\text{init}}-t}(Y_t)\} dt + \sqrt{2} dB_t, \quad Y_0 \sim \pi_{t_{\text{init}}}$$

where $p_s(y) = \int \mathcal{N}(y; e^{-s}x, (1 - e^{-2s})I) \pi(dx)$. By Tweedie’s formula, the intractable score $\nabla \log p_{t_{\text{init}}-t}(Y_t)$ can be written in terms of the posterior denoiser:

$$u_t(y) = \int x q_t(x | y) dx, \quad q_t(x | y) \propto \pi(x) \mathcal{N}(x; e^{t_{\text{init}}-t}y, (e^{2(t_{\text{init}}-t)} - 1)I),$$

so that the SDE becomes

$$dY_t = \left\{ \frac{e^{-2(t_{\text{init}}-t)} + 1}{e^{-2(t_{\text{init}}-t)} - 1} Y_t + \frac{2e^{-(t_{\text{init}}-t)}}{1 - e^{-2(t_{\text{init}}-t)}} u_t(Y_t) \right\} dt + \sqrt{2} dB_t.$$

Following the implementation of Grenioux et al. [9], RDMC discretizes the interval $[0, t_{\text{init}}]$ into T steps. At initialization, RDMC employs a *Langevin-within-Langevin* scheme to sample from $\pi_{t_{\text{init}}}$: using ULA where the score function is estimated based on DSI. In subsequent steps, RDMC simulates from the reverse SDE where the denoiser $u_t(y)$ is obtained by running MALA targeting $q_t(x | y)$.

The overall complexity of RDMC is $\mathcal{O}(NM(n_{\text{init}} + Tn))$ where N is the number of final samples, T is the number of iterative sampling steps, and the remaining factors are associated with score estimation: M is the number of MCMC chains, while n_{init} and n denote the number of MCMC transition steps in the initial and subsequent stages, respectively.

SLIPS [9]. Stochastic Localization via Iterative Posterior Sampling (SLIPS) relies on a stochastic observation process defined as:

$$Y_t = \alpha(t)X + \sigma W_t,$$

where $(W_t)_{t \geq 0}$ is a standard Brownian motion independent of $X \sim \pi$, and $\alpha(t)$ is a flexible denoising schedule function. To bypass the direct sampling requirement from π , SLIPS introduces a conditional denoiser defined by:

$$u_t(y) = \int x q_t(x | y) dx, \quad q_t(x | y) \propto \pi(x) \mathcal{N}\left(\frac{y}{\alpha(t)}, \frac{\sigma^2}{g(t)^2} I\right).$$

The corresponding SDE governing this observation process is:

$$dY_t = \dot{\alpha}(t)u_t(Y_t)dt + \sigma dB_t, \quad (37)$$

where $(B_t)_{t \geq 0}$ is another standard Brownian motion.

Similar to RDMC, the SLIPS algorithm approximates the dynamics defined by this SDE using an MCMC approach to estimate the conditional denoiser u_t or a related score function:

- The SLIPS initialization also involves a *Langevin-within-Langevin* procedure. Different from RDMC, SLIPS chooses the initialization time t_{init} such that both the marginal $\pi_{t_{\text{init}}}(y)$ and the posterior $q_{t_{\text{init}}}(x | y)$ are (approximately) log-concave, which they refer to as the “duality of log-concavity” assumption.
- In the subsequent steps, SLIPS integrates the observation process where the denoiser $u_t(Y_t)$ is estimated by MALA sampling from $q_t(x | y)$.

Similar to RDMC, SLIPS’ complexity is $\mathcal{O}(NM(n_{\text{init}} + Tn))$ where N is the number of final samples, T is the number of iterative sampling steps, and the remaining factors are associated with score estimation: M is the number of MCMC chains, while n_{init} and n denote the number of MCMC transition steps in the initial and subsequent stages, respectively.

SMS [33]. For a target π , Sequential Multimeasurement Sampler (SMS) draws M independent noisy observations at some noise scale $\sigma > 0$:

$$Y^m = X + \sigma Z^m, \quad Z^m \sim \mathcal{N}(0, I), \quad m = 1, \dots, M,$$

with $X \sim \pi$. For any $m \in \{1, \dots, M\}$, the posterior density of X given $y_{1:m}$ is

$$q_m(x | y_{1:m}) \propto \pi(x) \mathcal{N}(\bar{y}_{1:m}, \frac{\sigma^2}{m} I),$$

where $\bar{y}_{1:m} = (1/m) \sum_{i=1}^m y_i$. Its Bayes estimator

$$u_m(y_{1:m}) = \mathbb{E}[X | Y^{1:m} = y_{1:m}]$$

serves as a non-Markovian denoiser, and one shows that the law of $u_m(Y^{1:m})$ converges to π in W_2 at rate $O(\sigma \sqrt{d/m})$ [33].

To sample from π , one first simulates the entire M -tuple $Y^{1:M}$ and then returns $u_M(Y^{1:M})$. They employ a ‘Once-At-A-Time’ strategy: draw Y^1 via ULA, then sequentially sample each $Y^m | Y^{1:m-1}$ using MCMC targeting the conditional density of Y^m . Under mild assumptions this sequence of targets becomes increasingly log-concave in m , but the initial draw of Y^1 can be as challenging as sampling from π itself when σ is large. Although one can estimate scores via IS or inner-loop posterior MCMC, numerical results show a steep degradation in performance unless σ is carefully tuned—a manifestation of the same “duality of log-concavity” that forces a trade-off between ease of initialization and overall convergence as reported by Grenioux et al. [48].

The time complexity of SMS is $O(NTMn)$ for N final samples, T iterative sampling steps, n MCMC transition steps per sampling step, and M importance samples used for score estimation.

E.1.2 Implementation details and hyperparameter settings for the main experiments

We summarize the hyperparameter values used to tune RDSMC and its variants for the main experiments in Table 3, where these hyperparameters are explained in § B.3.3. The choices of score

Target	M	n	δ_{mcmc}	$t_{\text{start-resampling}}$	score est.	mcmc kernel
GMM ($d = 2, 4$)	{10, 100}	{1, 10}	{1.0}	{0.5, 0.8}	DSI	HMC
GMM ($d = 8 - 64$)	{10, 100}	{1, 10, 50}	{1.0}	{0.5, 0.8}	DSI	HMC
Rings	{100}	{1, 10}	{0.01, 0.05}	{0.5}	DSI	MALA
Funnel	{100}	{1, 10, 50}	{0.01, 0.05}	{0.5, 0.8}	DSI	MALA
Logistic Reg.	{10, 100}	{10, 50}	{0.01, 0.005}	{0.5, 0.8}	TSI	MALA

Table 3: Hyperparameter grid used for tuning RDSMC in the main experiments. We fix the number of sampling steps at $T = 100$, set $l = 1$ MCMC step per AIS transition, and use an ESS threshold of $\kappa_{\text{ess}} = 0.3$. Score estimator and MCMC kernel types are selected via a coarse grid search using validation metrics. RDSMC (IS) and RDSMC (Proposal) use the same grid with $\kappa_{\text{ess}} = 0$, excluding $t_{\text{start-resampling}}$ as it does not apply in these settings.

Target	AIS	SMC		SMS	
	$\delta_{\text{mcmc-init}}$	$\delta_{\text{mcmc-init}}$	κ_{ess}	δ_{mcmc}	δ_{γ}
GMM	{0.1, 0.5, 1.0}	{0.1, 0.5, 1.0}	{0.3, 1.0}	{0.03, 1.0}	{0.0625, 0.05}
Rings	{0.01}	{0.01}	{0.3, 1.0}	{0.03, 1.0}	{0.0625, 0.05}
Funnel	{0.01}	{0.01}	{0.3, 1.0}	{0.03, 1.0}	{0.0625, 0.05}
Logistic Reg.	{0.01}	{0.01}	{0.3, 1.0}	{0.03, 1.0}	{0.0625, 0.05}

Target	RDMC	SLIPS		
	$\exp\{t_{\text{init}}\}$	t_{final}	ϵ	$\delta_{\text{mcmc-init}}$
GMM	{0.95, 0.9, 0.8, 0.7}	{150, 300}	{0.03, 0.05, 0.1, 0.2, 0.4}	{0.1, 0.5, 1.0}
Rings	{0.95, 0.9, 0.8, 0.7}	{150, 300}	{0.1, 0.2, 0.4, 1.0, 1.2}	{1e-5}
Funnel	{0.95, 0.9, 0.8, 0.7}	{150, 300}	{0.1, 0.2, 0.4, 1.0, 1.2}	{1e-5}
Logistic Reg.	{0.95, 0.9, 0.8, 0.7}	{150}	{0.03, 0.05, 0.1, 0.2, 0.4}	{1e-5}

Table 4: Hyperparameter grid used for tuning baseline methods in the main experiments. AIS, SMC, RDMC, and SLIPS use $T = 1,000$ sampling steps, and SMS uses $K = 500$ noisy observations.

estimator and MCMC kernel types are determined by a coarse grid search using validation metrics; We primarily tune $M, n, \delta_{\text{mcmc}}$ and $t_{\text{start-resampling}}$, as described in Table 3.

The hyperparameter search grid for baseline methods is provided in Table 4. We largely follow the implementation of the official codebase of Grenioux et al. [9] (available at <https://github.com/h2o64/slips>). For the bi-modal GMM experiments, we tune key hyperparameters within a similar range to those used for RDSMC. For the Rings, Funnel, and Bayesian logistic regression tasks, we adopt the settings reported by Grenioux et al. [9].

We use the following target variance information to initialize AIS, SMC, and SLIPS. Crucially, RDMC and our method do not make use of this information.

We restate Assumption A0 from Grenioux et al. [9].

Assumption 1. (Log-concavity outside a compact). *There exist $R > 0$ and $\tau > 0$ such that π is the convolution of μ and $\mathcal{N}(0, \tau^2 \mathbf{I}_d)$, where μ is a distribution compactly supported on $\mathbb{B} = \mathbb{B}(\mathbf{m}_{\pi}, R)$, i.e., $\mu(\mathbb{R}^d \setminus \mathbb{B}) = 0$.*

The values of R and τ that approximately or exactly satisfy this assumption for different targets are provided in the corresponding experiment subsections.

We next discuss the hyperparameter settings for each of the baseline methods.

AIS. AIS uses $T = 1,000$ annealing steps. Each transition step uses an MALA kernel with an adaptive step size, initialized at $\delta_{\text{mcmc-init}}$, to maintain the acceptance ratio at 75%. Additionally, MALA runs 4 parallel chains, each with 32 MCMC steps. The initial proposal $\rho_0(x)$ is set to $\mathcal{N}(x | 0, R^2 + \tau^2)$.

The *only* tunable parameter we consider is $\delta_{\text{mcmc-init}}$.

SMC. SMC follows the same configuration as AIS, except it incorporates ESS-based resampling, introducing the normalized ESS threshold κ_{ess} as an additional hyperparameter (alongside $\delta_{\text{mcmc-init}}$).

RDMC. RDMC uses $T = 1,000$ discretization steps. To initialize $\pi_{t_{\text{init}}}$ in RDMC, the Langevin-within-Langevin algorithm is simulated using 16 MCMC steps and 4 MCMC chains. The chains are initialized with an IS approximation of the posterior powered by 128 particles. The initial sample is drawn from $\mathcal{N}(0, (1 - \exp\{-2t_{\text{init}}\})\mathbb{I}_d)$ and the initial step size is set to $(1 - \exp\{-2t_{\text{init}}\})/2$.

Subsequent steps use a MALA kernel for posterior sampling with adaptive step size to maintain the acceptance ratio at 75%, 4 parallel chains and 32 MCMC steps. We drop the first 50 MCMC samples to ignore the warm-up period in the estimation.

The only tunable parameter we consider is t_{init} .

SLIPS. SLIPS follows a similar initialization and posterior sampling scheme as RDMC, also with $T = 1,000$ discretization steps. However, instead of tuning the value of the initial sampling time t_{init} , SLIPS makes use of the target variance information and sets $\pi_{t_{\text{init}}}(x) := \mathcal{N}(x \mid 0, R^2/d + \tau^2)$.

SLIPS also features a few algorithmic subtleties.

- SLIPS uses a stochastic exponential integrator scheme to simulate from their observational SDE, where ours and RDMC consider the Euler Maruyama scheme.
- SLIPS discretizes the SDE using evenly spaced points in the log-SNR space, while our method and RDMC perform discretization in the time domain.
- SLIPS reuses the final MCMC samples from the previous step as the initialization for MCMC at the next step, promoting continuity across iterations.
- At the final step, SLIPS outputs the estimated denoiser as an approximate sample from the target π to align with standard stochastic localization literature. In contrast, our method and RDMC return a random sample generated from the approximated SDE dynamics.

We consider the following hyperparameters: (i) t_{final} the final integration time of Eq. (37), (ii) ϵ the initial time to determine the log-SNR-based discretization schedule, and (iii) $\delta_{\text{mcmc-init}}$, the initial step size for the MALA kernel.

SMS. We set the number of noisy observations M in SMS to $\lfloor T/2 \rfloor$ where $T = 1,000$, and use as many MCMC steps per noise level as SLIPS or RDMC. This choice of K ensures that the computational complexity of SMS is on par with other baseline methods. The Langevin steps are done using ULA as suggested by the authors.

We tune the step size δ_{mcmc} and the friction coefficient δ_γ using recommended values by the authors.

E.2 Bi-modal gaussian mixtures

Target. We consider a Gaussian mixture model (GMM) with two components in a d -dimensional space. The component means m_1, m_2 are randomly initialized from a uniform distribution over a box of width 80, centered at the origin. Each component has diagonal covariance with all diagonal values equal to $\sigma^2 = 2 \log 2$. The weights are fixed to $[w_1, w_2] = [0.1, 0.9]$ regardless of dimension d . Formally, the target density is

$$\pi(x) = w_1 \mathcal{N}(x \mid m_1, \sigma^2 \mathbb{I}_d) + w_2 \mathcal{N}(x \mid m_2, \sigma^2 \mathbb{I}_d). \quad (38)$$

Metrics. We compute the estimated weights by assigning samples to different components.

For a sample x , we assign it to the component $k \in \{1, 2\}$ with highest posterior probability value, which is computed as

$$p(x \text{ in component } k) = \frac{w_k \mathcal{N}(x \mid \mu_k, \sigma^2 \mathbb{I}_d)}{\sum_{j=1}^2 w_j \mathcal{N}(x \mid \mu_j, \sigma^2 \mathbb{I}_d)}.$$

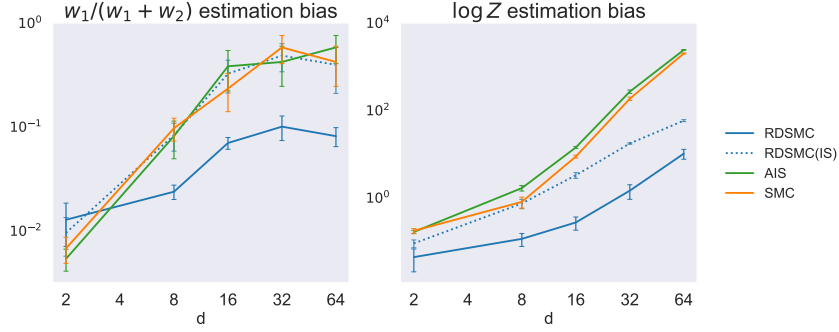


Figure 2: Estimation bias of weight ratio $w_1/(w_1 + w_2)$ and log normalization constant $\log Z$, with hyperparameters selected to minimize the $\log Z$ estimation bias. We observe that all methods exhibit monotonic trends in both bias metrics.

The weight estimates are then formulated as $\hat{w}_1 = \frac{1}{N} \sum_{i=1}^N \mathbf{1}\{x_i \text{ in component 1}\}$ and $\hat{w}_2 = 1 - \hat{w}_1$.

The weight estimation ratio bias is computed as $|\hat{w}_1/(\hat{w}_1 + \hat{w}_2) - w_1/(w_1 + w_2)| = |\hat{w}_1 - w_1|$.

The log normalization constant estimation bias is simply $|\hat{Z} - Z|$ where \hat{Z} is the estimated value, for method that computes it.

Additional implementation details. Assumption 1 are satisfied for $R = \max(w_1, w_2)\|m_1 - m_2\| = 0.9\|m_1 - m_2\|$, and $\tau = \sigma$. These values are used to initialize AIS, SMC, SMS, and SLIPS.

For RDSMC and its variants, we use DSI to estimate the score. The initial proposal distribution in Algorithm 3 is set to $\mathcal{N}(x_0 | x_t/\alpha_t, \sigma_t^2/\alpha_t^2)$.

Additional results. The hyperparameters used for results in Figure 1b are selected based on minimizing the estimation bias of weight ratio $w_1/(w_1 + w_2)$. Here, we also report results using hyperparameters tuned by minimizing the $\log Z$ bias in Figure 2. Results for RDSMC (Proposal), SMS, RDMC, and SLIPS are not included as they do not provide normalization constant estimate. The trends are largely similar, except that the $\log Z$ estimation bias curve appears monotonic.

E.3 Rings and Funnel distributions

Targets. The Rings distribution [9] is defined via an inverse polar reparameterization of a base distribution p_z , which is factorized into two independent univariate marginals p_r and p_θ :

- p_r is a mixture of four Gaussian distributions, each with mean located at integer radial positions $i + 1$ for $i \in \{0, 1, 2, 3\}$ and variance 0.15^2 .
- The angular component p_θ is uniformly distributed over $[0, 2\pi]$.

The Funnel distribution [34] is characterized by a hierarchical density structure in a 10-dimensional space, where the first dimension x_1 is drawn from a Gaussian distribution with zero mean and variance $\sigma^2 = 9$. The subsequent dimensions $x_{2:10}$ are conditionally Gaussian, with variances exponentially dependent on the first dimension. We follow Grenioux et al. [9] to use the following Funnel density

$$\pi(x_{1:10}) = \mathcal{N}(x_1; 0, \sigma^2)\mathcal{N}(x_{2:10}; 0, \exp(x_1)\mathbb{I}_9). \quad (39)$$

Metrics. The entropic regularized 2-Wasserstein distance between two distributions μ and ν is defined by

$$W_{2,\varepsilon}(\mu, \nu) = \inf\left\{\int_{\mathbb{R}^d \times \mathbb{R}^d} \|x_1 - x_0\|^2 d\pi(x_0, x_1) - H(\pi) : \pi_0 = \mu, \pi_1 = \nu\right\}^{1/2}, \quad (40)$$

where $\varepsilon > 0$ is a regularization hyper-parameter and $H(\pi) = -\int_{\mathbb{R}^d \times \mathbb{R}^d} \log \pi(x_0, x_1) d\pi(x_0, x_1)$ refers to as the entropy of π . We evaluate the quality of sampling with regularization $\varepsilon = 0.05$ via POT library [49].

Total Variation Distance (TVD) measures the discrepancy between the true and model-generated distributions by comparing their marginal histograms within a bounded region.

Let $\hat{\mu}_i$ and $\hat{\nu}_i$ represent the probability mass in the i -th bin for the true and generated distributions, respectively. We compute the TVD as follows

$$\text{TVD} = \frac{1}{2} \sum_i |\hat{\mu}_i - \hat{\nu}_i|,$$

For the radius TVD, we generate the histogram of the radius samples using 256 uniform bins over the interval $[0, 8]$. For the angle TVD, we generate the histogram of angle samples using 256 uniform bins over the interval $[-\pi, \pi]$.

The Kolmogorov-Smirnov distance (KSD) between two distributions μ and ν is defined by

$$\text{KSD}(\mu, \nu) = \sup_{x \in \mathbb{R}^d} \|F_\mu(x) - F_\nu(x)\|, \quad (41)$$

where F_μ and F_ν denotes the cumulative distribution function of μ and ν respectively. We evaluate the 10-dimensional Funnel samples using the sliced version from [48, Appendix D.1].

Additional implementation details. For both targets, we use DSI to estimate the score. On Rings, we choose $R = 4, \tau = 0.15$ that satisfy Assumption 1 to initialize AIS, SMC, SMS, and SLIPS; and on Funnel, we use $R = 2.12, \tau = 0.0$, following the implementation of Grenioux et al. [9].

On Rings, we set the initial proposal distribution in Algorithm 3 for RDSMC and its variants to $\mathcal{N}(x_0 | x_t/\alpha_t, \sigma_t^2/\alpha_t^2)$. On Funnel, the above choice would render numerical instability when t is large. Hence we use $\mathcal{N}(x_0 | x_t, \sigma_t^2/\alpha_t^2)$ as the proposal for the AIS procedure.

E.4 Bayesian logistic regression

Targets. We consider four Bayesian logistic regression datasets: Credit and Cancer [35], Ionosphere [36] and Sonar [37].

- Credit [35]: this dataset addresses binary classification of individuals as good or bad credit risks. It contains 1000 data points with 25 standardized features.
- Cancer [35]: this dataset involves classifying recurrence events in breast cancer. It consists of 569 data points in a 31-dimensional standardized feature space.
- Ionosphere [36]: this dataset classifies radar signals passing through the ionosphere into good or bad categories. It features 351 data points with dimensionality $d = 35$.
- Sonar [37]: this dataset differentiates sonar signals reflected from metal cylinders versus cylindrical rocks. It includes 208 data points with $d = 61$ standardized features.

We consider a training dataset $\mathcal{D} = \{(x_j, y_j)\}_{j=1}^M$ where $x_j \in \mathbb{R}^d$ and $y_j \in \{0, 1\}$ for all $j \in \{1, \dots, M\}$. A Bayesian logistic regression model consists of the following

$$p(w, b) = \mathcal{N}(w; 0, \mathbf{I}_d) \mathcal{N}(b; 0, (2.5)^2) \quad (42)$$

$$p(y | x; w, b) = \text{Bernoulli}(y; \sigma(x^\top w + b)) \quad (43)$$

where $w \in \mathbb{R}^d$ is a weight vector, $b \in \mathbb{R}$ is an intercept, and σ is the sigmoid function.

The target distribution we are interested in is the posterior distribution

$$p(w, b | \mathcal{D}) \propto p(\mathcal{D} | w, b) p(w, b) = \prod_{j=1}^M p(y_j | x_j; w, b) p(w, b). \quad (44)$$

Metric. Following Grenioux et al. [9], we use the following definition of the predictive log-likelihood given a test dataset $\mathcal{D}_{\text{test}}$:

$$\frac{1}{N} \sum_{i=1}^N \sum_{(x, y) \in \mathcal{D}_{\text{test}}} \log p(w_i, b_i) + \log p(y | x; w_i, b_i) \quad (45)$$

where $\{w_i, b_i\}_{i=1}^N$ are posterior samples.

Additional implementation details. On all tasks, we use $R = 2.5, \tau = 0.0$ in Assumption 1 to initialize AIS, SMC, SMS, and SLIPS following the implementation of Grenioux et al. [9].

For RDSMC and its variants, we use TSI to estimate the score and clip the norm of the estimated score within 20 to improve numerical stability. We use $\mathcal{N}(x_0 | x_t/\alpha_t, \sigma_t^2/\alpha_t^2)$ as the initial proposal distribution in the AIS-based score estimation procedure.

E.5 Ablation experiments

In our main experiments, baseline methods follow the implementation of Grenioux et al. [9] which use more discretization steps T compared to our method, and result in different runtimes. Additionally, AIS, SMC and SLIPS use target variance information while RDSMC does not.

In this section, we conduct ablation studies to control for these factors and evaluate performance under comparable computational budgets. We discuss the hyperparameter settings in § E.5.1. We present the results for the targets in the main experiments with the new hyperparameter settings in § E.5.2.

In addition, we include an empirical comparison to the Particle Denoising Diffusion Sampler [11] in § E.5.3.

E.5.1 Hyperparameter settings

To enable fair comparisons under similar computational budgets, we fix the compute budget for RDSMC and align the hyperparameters of SLIPS, RDMC, and SMS accordingly, since these methods have comparable computational complexity; however, algorithmic differences lead to variations in runtime. For AIS and SMC, we adjust their hyperparameters to achieve total runtimes comparable to that of RDSMC.

In addition, only SLIPS and SMS use target scalar variance to initialize their samplers, while other methods including RDSMC do not access this information.

We summarize hyperparameter settings for each method below.

RDSMC.

- Use $T = 100$ uniform discretization timesteps
- Use AIS score estimator based on the DSI, and MALA as the MCMC kernel in AIS
- Use an adaptive MCMC step size, similar to that used in the baseline SLIPS, AIS, and SMC methods (see description in § B.3.3). This adaptive strategy differs from the fixed step size employed in the main experiments which requires tuning. The initial MCMC step size is 1 for GMM targets and 0.05 for others.
- Use $M = 100$ AIS importance samples
- Use $n = 50$ AIS annealing steps
- Use $m = 1$ MCMC transition per AIS step
- Use $\kappa_{\text{ess}} = 0.3$ for the ESS-based resampling threshold
- The *only* tunable hyperparameter is the starting step for resampling, $t_{\text{start-resampling}}$, which we vary in $\{0, 0.1, 0.2, \dots, 1.0\}$ unless otherwise specified. Recall that we apply resampling at step t when $t \leq t_{\text{start-resampling}}$ and the normalized ESS $< \kappa_{\text{ess}}$.

We treat RDSMC (IS) as a special case of RDSMC with $t_{\text{start-resampling}} = 0$, which is included within the generic RDSMC framework as part of hyperparameter tuning. The final hyperparameter values tuned by validation metrics are reported in Table 5.

RDSMC (Proposal) uses the same configuration as RDSMC except that no resampling or weighting is applied throughout the sampling process.

AIS and SMC. To generate N final samples, recall that the computational complexity of AIS and SMC is $O(NTn)$ for T annealing steps and n MCMC transitions per step; in contrast, RDSMC’s

Target	start resampling time ($t_{\text{start-resampling}}$)
GMM ($d = 2$)	0.2
GMM ($d = 4$)	0.6
GMM ($d = 8$)	0.4
GMM ($d = 16$)	0.2
GMM ($d = 32$)	0.1
GMM ($d = 64$)	0.4
Rings	0.1
Funnel	1.0
Credit	0.9
Cancer	0.6
Ionosphere	0.7
Sonar	1.0

Table 5: Ablation experiments: final hyperparameter settings for RDSMC, selected by target-dependent validation metrics.

Target	# of annealing steps (T)	# of MCMC transitions per step (n)
GMM ($d = 2, 4, 8$)	100	100
GMM ($d = 16$)	150	100
GMM ($d = 32$)	240	100
GMM ($d = 64$)	400	100
Rings	100	70
Funnel	100	100
Credit	1000	140
Cancer	1000	90
Ionosphere	1000	70
Sonar	1000	60

Table 6: Ablation experiments: final hyperparameter settings for AIS and SMC, tuned to achieve comparable runtime to RDSMC (with $T = 100$ time steps, $M = 100$ AIS importance samples, and $n = 50$ AIS annealing steps) on a single NVIDIA A100 GPU (40 GB memory). While the M importance samples in RDSMC can be processed in parallel, computation can still result in slower performance on a single device. We therefore increase T and n for AIS and SMC to match the runtime of RDSMC.

complexity is $\mathcal{O}(NTMn)$ for T discretization steps, M AIS importance samples, n AIS annealing steps (with a minor abuse of notation).

While the M AIS importance samples in RDSMC can be processed in parallel, computation can still result in slower runtime on a single device. Therefore, we adjust the number of annealing steps T and the number of MCMC transitions per step n to ensure that the total runtime on a single NVIDIA A100 GPU (40 GB memory) is comparable to that of RDSMC. The resulting hyperparameter values are provided in Table 6.

Additionally, in contrast to the main experiments following Grenioux et al. [9], we do *not* use the target variance to initialize the initial proposal in AIS and SMC. Instead, we use the initial proposal $\mathcal{N}(0, 1)$ which coincides with the base distribution of RDSMC. We use the same adaptive MCMC step size strategy as in RDSMC. For SMC, the ESS-based resampling threshold is set to 0.3.

Other aspects of AIS and SMC are the same as in the main experiments.

SLIPS and RDMC. We match the computational budget of each score estimation step to that of RDSMC. Specifically, both SLIPS and RDMC use $T = 100$ discretization steps; in every step, they use $M = 100$ parallel MCMC chain, each with $n = 50$ transitions, for score estimation. Consequently, the asymptotic complexity of SLIPS and RDMC (after the initialization stage) is the same as that of RDSMC, which is $\mathcal{O}(NTMn)$ to produce N final samples.

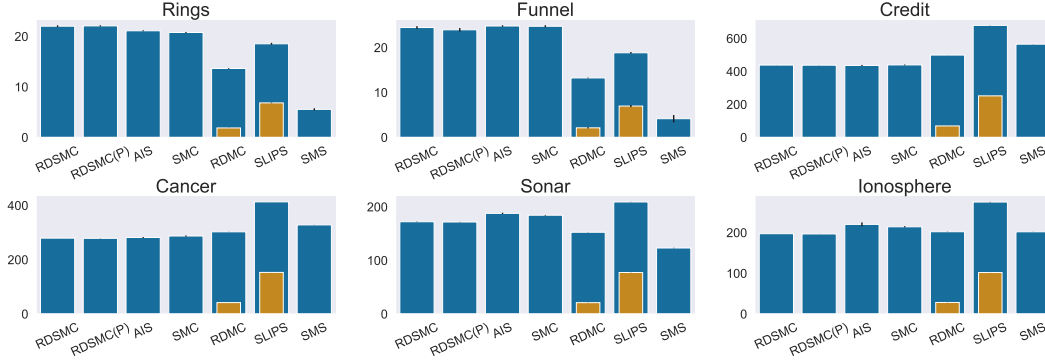


Figure 3: Ablation experiments: runtimes (in seconds) for all methods across different targets. Each blue bar represents the total wall-clock time averaged over 10 random seeds with error bar denoting 2 standard errors, measured on a single NVIDIA A100 GPU (40 GB). For RDMC and SLIPS, we also include the initialization time indicated by the orange bars. RDSMC(P) denotes RDSMC (Proposal). The GMM results are reported separately in the final panel of Figure 4. AIS and SMC are configured to achieve runtimes comparable to RDSMC. While RDMC, SLIPS and SMS have the same asymptotic complexity of RDSMC, their actual runtimes differ due to algorithmic differences.

However, because SLIPS and RDMC require additional computation for initialization and their score estimation relies on MCMC, whereas RDSMC starts from the base distribution and uses AIS for score estimation, the overall runtimes of these methods differ.

Other aspects of SLIPS and RDMC are the same as in the main experiments

SMS. We use $T = 100$ steps, $n = 50$ MCMC transitions per sampling step and $M = 100$ importance samples for score estimation. Other aspects of SMS are the same as in the main experiments.

E.5.2 Ablation experiment results

We revisit the targets studied in the main experiment using the new hyperparameter settings and summarize the results. Each experiment is run with 10 random seeds, and hyperparameters are selected using the corresponding validation metrics.

Runtime. The overall runtimes for all methods across all targets are shown in Figure 3, except for the GMM targets, which are presented in the final panel of Figure 4.

We note that AIS and SMC are manually configured to achieve runtimes comparable to RDSMC. While RDMC, SLIPS and SMS have the same asymptotic complexity of RDSMC, their actual runtimes differ due to algorithmic differences. In GMM (with varying d), Rings, and Funnel, we observe shorter runtimes for RDMC, SLIPS, and SMS compared to RDSMC. In contrast, for Credit, Cancer, Sonar, and Ionosphere, SLIPS tends to have a longer runtime. Notably, the initialization phase of RDMC and SLIPS accounts for a substantial portion of their total runtime.

Bi-modal GMM. We report the results in Figure 4. In the first two panels, we observe that for both the weight ratio $w_1/(w_1 + w_2)$ and the log normalization constant $\log Z$, RDSMC consistently outperforms the other methods. These results are consistent with the findings in the main experiments in Figure 1, despite a different hyperparameter setting. The last panel summarizes the runtime comparison.

The optimal hyperparameters for each method are selected based on the lowest estimation bias of the weight ratio, consistent with the procedure used in the main experiments.

Rings and Funnel. We report the results in Table 7. On synthetic targets, AIS and SMC achieve the lowest average Radius TVD and $\log Z$ bias on Rings and lowest average $\log Z$ bias on Funnel, while RDSMC achieves comparable results on these metrics and the lowest average Sliced KSD on Funnel.

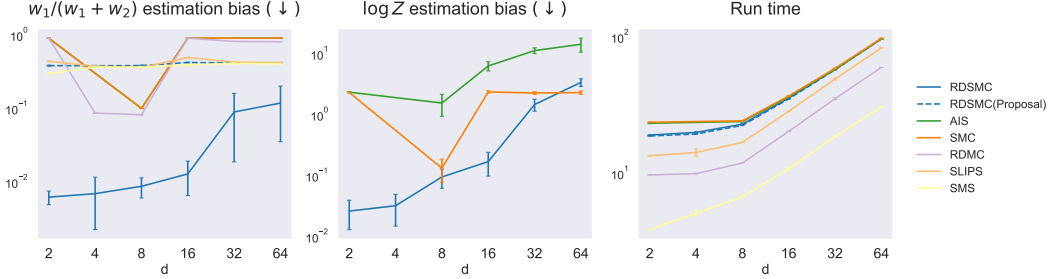


Figure 4: Ablation experiments: estimation bias of weight ratio $w_1/(w_1 + w_2)$ (left) and log-normalization constant $\log Z$ (middle), and runtime (in seconds, right) versus dimension d . Results are averaged over 10 seeds with error bars showing one standard error. Note that SMS, RDMC, and SLIPS do not provide estimates of $\log Z$. For both metrics, the estimation bias increases with d for all methods, while RDSMC consistently outperforms the baselines. The runtime for RDSMC (including the Proposal variant). SMC and AIS are configured for comparable runtime of RDSMC, whereas SLIPS, RDMC, and SMS exhibit shorter runtimes owing to algorithmic differences, despite having the same asymptotic complexity as RDSMC.

Algorithm	Rings		Funnel	
	Radius TVD \downarrow	$\log Z$ bias \downarrow	Sliced KSD \downarrow	$\log Z$ bias \downarrow
RDSMC	0.118 ± 0.002	0.013 ± 0.004	$0.075 \pm 0.005^*$	0.286 ± 0.068
RDSMC(Proposal)	0.091 ± 0.003	N/A	0.327 ± 0.033	N/A
RDMC	0.440 ± 0.003	N/A	0.129 ± 0.000	N/A
SLIPS	0.279 ± 0.003	N/A	0.076 ± 0.001	N/A
AIS	0.088 ± 0.003	$0.004 \pm 0.002^*$	0.087 ± 0.002	0.173 ± 0.010
SMC	$0.088 \pm 0.002^*$	0.006 ± 0.002	0.082 ± 0.004	$0.169 \pm 0.012^*$
SMS	0.282 ± 0.010	N/A	0.161 ± 0.000	N/A

Table 7: Ablation experiments: Rings and Funnel targets (mean \pm standard error over 10 seeds). * indicates the best average results and bold indicates 95% confidence interval overlap with that of the best average result. AIS and SMC achieve the lowest average Radius TVD and $\log Z$ bias on Rings, and the lowest $\log Z$ bias on Funnel, with RDSMC remaining comparable when accounting for standard errors. RDSMC achieves the lowest Sliced KSD on Funnel.

Note that these observations differ slightly from those in the main experiments (Table 1) due to changes in the hyperparameter settings. In particular, AIS and SMC no longer use target-variance scaling for initialization, which appears to improve their performance in this case.

In this new setting, AIS and SMC demonstrate more robust overall performance. While RDSMC remains competitive, it exhibits greater variability in the reported metrics (indicated by the larger standard errors). Nevertheless, RDSMC tends to outperform diffusion-based MC samplers that do not have SMC correction, including its Proposal variant, SLIPS, and RDMC.

The optimal hyperparameters for each method are selected based on the lowest Radius TVD for Rings and lowest Sliced KSD for Funnel, consistent with the procedure used in the main experiments.

Finally, we note that for RDSMC on the Rings target, when the hyperparameter $t_{\text{start-resampling}} > 0.8$, the magnitude of the estimated $\log Z$ becomes significantly larger than when $t_{\text{start-resampling}} \leq 0.8$. For this reason, we tune $t_{\text{start-resampling}} \in \{0, 0.1, \dots, 0.8\}$, within which the estimated $\log Z$ values remain consistent.

Bayesian logistic regression. Different from the main experiments in Table 8, we consider a different metric Test LPPD, the log pointwise predictive density on the test set, defined as follows

$$\text{Test LPPD} = \sum_{(x,y) \in \mathcal{D}_{\text{test}}} \log \left(\int p(y_i | x_i; w, b) p(w, b | \mathcal{D}) dw, b \right) \quad (46)$$

Test LPPD \uparrow	Credit ($d = 25$)	Cancer ($d = 31$)	Ionosphere ($d = 35$)	Sonar ($d = 61$)
RDSMC	-94.54 \pm 1.34	-10.59 \pm 0.45	-25.97 \pm 0.73	-18.54 \pm 0.28
RDSMC(Proposal)	-94.62 \pm 0.06	-50.24 \pm 0.16	-24.87 \pm 0.02*	-18.91 \pm 0.01
RDMC	-138.22 \pm 0.35	-78.03 \pm 0.12	-44.16 \pm 0.07	-28.64 \pm 0.03
SLIPS	-92.42 \pm 0.02*	-10.41 \pm 0.01	-25.22 \pm 0.01	-18.40 \pm 0.01*
AIS	-92.91 \pm 0.44	-10.13 \pm 0.07	-25.09 \pm 0.02	-18.41 \pm 0.01
SMC	-92.55 \pm 0.05	-10.13 \pm 0.01*	-25.09 \pm 0.02	-18.41 \pm 0.01
SMS	-98.00 \pm 0.27	-20.47 \pm 0.16	-26.17 \pm 0.10	-23.29 \pm 0.08

Table 8: Ablation experiments: Bayesian logistic regression with test log pointwise predictive density (Test LPPD, with mean \pm standard error) averaged over 10 seeds. * indicates the best average result and bold indicates 95% confidence interval overlap with that of the best average result. RDSMC, AIS, SMC, and SLIPS achieve the best overall performance. RDSMC outperforms RDSMC (Proposal) and RDMC in most cases, highlighting the effectiveness of the SMC correction.

where the likelihood $p(y_i | x_i; w, b)$ is defined in Eq. (43) and the posterior $p(w, b | \mathcal{D})$ is defined in Eq. (44).

We use final (weighted) samples from each method to approximate the Test LPPD in Eq. (46).

We report the results in Table 8. We observe that RDSMC, AIS, SMC, and SLIPS achieve the best overall performance. Compared to SLIPS, RDSMC does not require target-variance-based initialization. Moreover, RDSMC outperforms RDSMC (Proposal) and RDMC in most cases, highlighting the effectiveness of the SMC correction. However, we observe that results for RDSMC exhibit large variance, as the case in the main experiments from Table 2.

The optimal hyperparameters for each method are selected based on the highest LPPD on a heldout validation set, computed analogously to the Test LPPD.

E.5.3 Comparison to Particle Denoising Diffusion Sampler on the Funnel target

Finally, we present a comparison to the Particle Denoising Diffusion Sampler (PDDS) [11], which is also a diffusion-based SMC sampler. However, unlike RDSMC, PDDS requires training.

We evaluate PDDS on the Funnel target using 10 random seeds. Experiments are conducted on an NVIDIA RTX A6000 GPU, whereas our previous experiments use an NVIDIA A100 GPU. In addition, PDDS is implemented in JAX (following the official implementation at https://github.com/angusphillips/particle_denoising_diffusion_sampler#), while RDSMC and the other baselines are implemented in PyTorch.

PDDS requires approximately 82.63 ± 0.43 seconds for training and 15.08 ± 0.073 seconds for final sampling of 4096 particles, resulting in a total runtime of about 97.70 ± 0.47 seconds (reported as mean \pm standard error). The runtimes of our method and other training-free baselines are reported in Figure 3, which are all below 25 seconds. However, due to differences in hardware and software frameworks, PDDS’s runtime is not directly comparable to those of the previous experiments.

PDDS achieves a $\log Z$ bias of 0.26 ± 0.04 and a mean Sliced KSD of 0.10 ± 0.00 . Compared with the results in Table 7, PDDS exhibits a slightly lower average $\log Z$ bias than RDSMC, but higher than AIS and SMC. Its Sliced KSD is also higher than that of RDSMC, AIS, and SMC.